NASA TECHNICAL NOTE

NASA TN D-6821

NASA TN D-6821

EFFECTS OF BODY SHAPE ON THE AERODYNAMIC CHARACTERISTICS OF AN ALL-BODY HYPERSONIC AIRCRAFT CONFIGURATION AT MACH NUMBERS FROM 0.65 TO 10.6

by Walter P. Nelms, Jr.

Ames Research Center
Moffett Field, Calif. 94035

NATIONAL AERONAUTICS AND SPACE ADMINISTRATION • WASHINGTON, D. C. • MAY 1972

1. Report No.	2. Government Accession No.	3. Recipient's Catalog No.
NASA TN D-6821		

4. Title and Subtitle	5. Report Date
EFFECTS OF BODY SHAPE ON THE AERODYNAMIC CHARACTERISTICS OF AN ALL-BODY HYPERSONIC AIRCRAFT CONFIGURATION AT MACH NUMBERS FROM 0.65 TO 10.6	May 1972
	6. Performing Organization Code
7. Author(s)	8. Performing Organization Report No.
Walter P. Nelms, Jr.	A-4297
	10. Work Unit No.
9. Performing Organization Name and Address	136-13-05-01-00-21
NASA Ames Research Center Moffett Field, Calif. 94035	11. Contract or Grant No.
	13. Type of Report and Period Covered
12. Sponsoring Agency Name and Address	Technical Note
National Aeronautics and Space Administration Washington, D. C. 20546	14. Sponsoring Agency Code

15. Supplementary Notes

16. Abstract

An experimental investigation was conducted to determine the effects of several variations in body shape on the aerodynamic characteristics of an all-body hypersonic aircraft configuration. The basic configuration had a delta planform with an elliptic cone forebody and an afterbody of elliptic cross section terminating in a straight-line trailing edge. Variations in body shape included the ratio of maximum cross-sectional to body planform area (0.0935 and 0.0625), body leading-edge sweep (75° and 80°), and forebody length ratio (0.667 and 0.750). In addition, the effects of a thin wing (1.5 percent thick) mounted on one of the bodies was investigated, and the aerodynamic characteristics of just the forebodies of two of the configurations were determined. The models had no stabilizing surfaces or propulsion system packages. Ranges of angle of attack (−4° to +15°) and angle of sideslip (−4° to +8°) were investigated. The results indicate that of the four complete bodies, the configuration with the lowest ratio of cross-sectional to body planform area had the highest maximum lift-drag ratio and the greatest level of longitudinal stability at most Mach numbers. All the configurations had positive longitudinal stability near maximum lift-drag ratio at most Mach numbers. With exception of the lowest subsonic Mach numbers, changes in body sweep angle and in forebody length ratio had only minor effects on maximum lift-drag ratio.

17. Key Words (Suggested by Author(s))	18. Distribution Statement
Hypersonic aircraft Hypersonic flight Lift-drag ratio Longitudinal stability Aerodynamic characteristics Wind tunnel models	Unclassified – Unlimited

19. Security Classif. (of this report)	20. Security Classif. (of this page)	21. No. of Pages	22. Price*
Unclassified	Unclassified	61	$3.00

*For sale by the National Technical Information Service, Springfield, Virginia 22151

NOTATION

The longitudinal force and moment coefficients are referred to the stability-axis system, and the lateral-directional coefficients are referred to the body-axis system. All force and moment coefficients are based on a reference area defined as the total planform area for the respective models. For all the bodies, the moment reference center is located on the body centerline at 32.5 percent of the mean aerodynamic chord, which corresponds to the 55.0 percent point of the body length.

a_π	semimajor axis of maximum cross section
a.c.	longitudinal aerodynamic center defined at $\left(\frac{L}{D}\right)_{max}$, percent $\bar{c}$
A_b	model balance cavity area (4.38 cm^2 for all models)
b	span (measured between body tips)
b_π	semiminor axis of maximum cross section
c	local chord length of airfoil section
$\bar{c}$	mean aerodynamic chord $\left(\frac{2}{3}l\right)$
C_A	axial-force coefficient, $C_{A_{total}} - C_{A_b}$
C_{A_b}	balance cavity axial-force coefficient, $\frac{(p_\infty - p_b)A_b}{qS}$
$C_{A_{total}}$	total measured axial-force coefficient
C_D	drag coefficient, $\frac{drag}{qS}$
C_{D_0}	drag coefficient at zero lift
C_L	lift coefficient, $\frac{lift}{qS}$
C_{L_0}	lift coefficient at zero angle of attack
C_{L_α}	lift-curve slope at zero lift, $\frac{\partial C_L}{\partial \alpha}$, per deg
C_l	rolling-moment coefficient, $\frac{rolling\ moment}{qSb}$
C_m	pitching-moment coefficient, $\frac{pitching\ moment}{qS\bar{c}}$

C_{m_0}	pitching-moment coefficient at zero lift
C_N	normal-force coefficient, $\frac{\text{normal force}}{qS}$
C_n	yawing-moment coefficient, $\frac{\text{yawing moment}}{qSb}$
C_Y	side-force coefficient, $\frac{\text{side force}}{qS}$
$\frac{L}{D}$	lift-drag ratio
$\left(\frac{L}{D}\right)_{max}$	maximum lift-drag ratio
l	body length
l_π	forebody length (measured from nose to maximum cross section)
M	free-stream Mach number
p_b	model balance cavity pressure
p_∞	free-stream static pressure
q	free-stream dynamic pressure
R_l	Reynolds number based on body length
S	reference area $\left(\text{body planform area defined as } \frac{lb}{2}\right)$
S_π	maximum cross-sectional area
t	maximum thickness of airfoil section
$\frac{t}{c}$	airfoil thickness-to-chord ratio
V	total volume
x	longitudinal coordinate, measured rearward from model nose
y	spanwise coordinate, measured from body centerline
z	vertical coordinate, measured from body centerline
α	angle of attack (referred to body centerline), deg

β	angle of sideslip (referred to body centerline), deg
Λ	body (or wing) sweepback angle, deg

EFFECTS OF BODY SHAPE ON THE AERODYNAMIC CHARACTERISTICS OF AN ALL–BODY HYPERSONIC AIRCRAFT CONFIGURATION AT MACH NUMBERS FROM 0.65 TO 10.6

Walter P. Nelms, Jr.

Ames Research Center

SUMMARY

An experimental investigation was conducted at Mach numbers from 0.65 to 10.61 to determine the effects of several variations in body shape on the aerodynamic characteristics of an all-body hypersonic aircraft configuration. The basic configuration had a delta planform with an elliptic cone forebody and an afterbody of elliptic cross section terminating in a straight-line trailing edge. Variations in body shape included the ratio of maximum cross-sectional to body planform area (0.0935 and 0.0625), body leading-edge sweep (75° and 80°), and forebody length ratio (0.667 and 0.750). In addition, the effects of a thin wing (1.5 percent thick) mounted on one of the bodies was investigated, and the aerodynamic characteristics of just the forebodies of two of the configurations were determined. The models had no stabilizing surfaces or propulsion system packages. Ranges of angle of attack (−4° to +15°) and angle of sideslip (−4° to +8°) were investigated.

The results indicate that, of the four complete bodies, the configuration with the lowest ratio of cross-sectional to body planform area had the highest maximum lift-drag ratio and the greatest level of longitudinal stability at most Mach numbers of the test. For the selected moment reference centers, all configurations had positive longitudinal stability near maximum lift-drag ratio at most Mach numbers of the test. Except at the lowest subsonic Mach numbers, changes from the nominal configuration in body sweep angle and in forebody length ratio had only minor effects on maximum lift-drag ratio. The addition of thin wings, or strakes, to the alternate sweep configuration increased maximum lift-drag ratio at most speeds, and increased longitudinal stability at the hypersonic Mach numbers.

INTRODUCTION

Several configurations have been investigated both analytically and experimentally in a program at Ames Research Center to provide preliminary aerodynamic characteristics of hypersonic aircraft configurations suitable for cruise, boost, and military missions (refs. 1–9). Among these configurations was an all-body concept considered in the analytical studies of references 7 through 9. Results of wind tunnel tests of the nominal configuration derived from these analytical studies are presented in reference 10, which primarily includes stabilizing and control surface effectiveness as well as results of component buildup. During these wind tunnel tests, the effects of several alterations in the body shape and the effects of adding thin wings to one of the bodies were investigated. This was undertaken as a preliminary exploration of means to improve the

aerodynamic efficiency of this particular all-body concept, as well as to provide additional experimental data to be used in the assessment of various theoretical techniques for use on this configuration. The present report includes the results from these tests.

The experimental investigation was conducted in the Ames 6– by 6–Foot Supersonic and the 3.5–Foot Hypersonic Wind Tunnels over a Mach number range from 0.65 to 10.61. The Reynolds number was held constant at 8.2×10^6/m for most of the tests; at Mach numbers 2.00 and 10.61, the Reynolds number was limited to 4.9×10^6/m. Angles of attack ranged from −4° to +15°, and angles of sideslip ranged from −4° to +8°.

MODEL

Figure 1 presents a drawing of the various models, and indicates the appropriate identification symbols (B_1, B_2 etc.) and shape parameters for each configuration. The equation defining the maximum cross section of the models is also shown in figure 1. Pertinent model dimensions and areas are listed in table 1. Figure 2 presents photographs of the models.

Reference 10 includes the aerodynamic characteristics of the nominal body (B_1) together with the effectiveness of stabilizing and control surfaces and component buildup results. The present report considers the effects of variations in body shape from the nominal configuration and also includes the effects of thin wings on one of the bodies. In addition, the aerodynamic characteristics of the forebodies of two of the configurations are presented. The models used for these tests had no stabilizing surfaces or propulsion system packages.

The nominal configuration (fig. 1) had a delta planform with an elliptic cone forebody and an afterbody of elliptic cross section. The afterbody ellipticity continuously increased with body station forming a smooth transition from the end of the forebody to a straight-line trailing edge. Variations in the body shape from the nominal were accomplished by individually varying three parameters as identified in reference 9: (1) the ratio of maximum cross-sectional to body planform area ("fatness ratio") S_π/S; (2) the body sweepback angle Λ; and (3) the forebody length ratio l_π/l. It should be noted that for the configurations considered herein, the longitudinal location of the forebody-afterbody breakpoint and the maximum cross-sectional area coincide. In comparison to the nominal body (B_1), configuration B_2 had an alternate fatness ratio, configuration B_3 had an alternate sweep, and configuration B_4 had an alternate forebody length ratio (fig. 1). The volumes of the four configurations were equal; this accounts for the differences in body length (l) shown in figure 1 and table 1.

A thin wing, or strake, of 75° sweepback angle was provided for mounting on the centerline of configuration B_3 as indicated in figure 1. The wing, with a maximum thickness-to-chord ratio of 1.5 percent, had a symmetrical wedge-slab-wedge airfoil section with ridge lines at 30 and 70 percent of the local chords.

The forebodies of two of the configurations were tested alone to provide data in the form of a configuration buildup for comparison with theory. Configuration B_5 was the forebody of the nominal configuration (B_1), and B_6 was the forebody of the alternate sweep configuration (B_3).

TESTS

Experimental data were obtained in air in two Ames wind tunnels over a Mach number range of 0.65 to 10.61. The 6– by 6–foot supersonic tunnel is a closed-circuit, continuous-flow facility with a sliding block nozzle and a slotted wall test section; in this tunnel, the Mach number was varied from 0.65 to 2.00. Mach numbers of 5.37, 7.38, and 10.61 were obtained in the 3.5–foot hypersonic tunnel, which uses interchangeable nozzles; this tunnel is a blowdown facility in which incoming air is preheated by a pebble-bed heater to prevent liquefaction of air in the test section. The stagnation temperature was maintained at about 720° K for Mach numbers of 5.37 and 7.38 and at about 1050° K for Mach number 10.61. Data were obtained at a constant Reynolds number of 8.2×10^6/m at all Mach numbers except at 2.00 and 10.61, where the unit Reynolds number was limited to 4.9×10^6/m because of wind tunnel limitations.

Except for configurations B_5 and B_6, the models were sting-mounted through the aft upper surface of the body; this method of support was used so as to have an undisturbed lower body surface for testing at hypersonic speeds. For tests of the two forebodies alone (B_5 and B_6), the sting exited through the base. Force and moment measurements were made with an internally mounted, six-component strain-gage balance. Test angles of attack ranged nominally from −4° to +15°, and angles of sideslip ranged nominally from −4° to +8°. The angles of attack and sideslip were corrected for wind tunnel flow misalinement and for balance and sting deflections caused by the aerodynamic loads. Balance cavity pressure was measured and the drag data were adjusted to a condition corresponding to free-stream static pressure in the cavity. Table 2 is a list of the balance cavity axial-force coefficients subtracted from the drag measurements of the nominal configuration (B_1); similar corrections were applied to the data of the other configurations.

For these particular tests, boundary-layer transition was not fixed on the models; reference 10 discusses the results of studies conducted to establish the drag level of the nominal configuration. On the basis of these studies, it can be concluded that the boundary layers on the present models were mostly laminar at the hypersonic Mach numbers of the test.

A moment reference center of 0.325 $\bar{c}$ (0.55l) was selected for presenting the data in order to be consistent with the results of reference 10. From mission studies involving this configuration (refs. 7–9), it appears that the center of gravity would be located aft of this selected point at approximately 0.445 $\bar{c}$ (0.63l).

Based on repeatability of the data and known precision of the measuring equipment the test Mach numbers 0.65–2.00 and 5.37–10.6 are considered accurate within ±0.01 and ±0.05, respectively; the corresponding dimensionless aerodynamic coefficients are considered accurate within ±2 and ±3 percent, respectively. The angles of attack and sideslip are considered to be accurate within ±0.2°.

RESULTS AND DISCUSSION

Complete Bodies

Longitudinal characteristics– The longitudinal aerodynamic characteristics of the complete bodies (with forebody and afterbody but without stabilizing surfaces) are presented as a function of lift coefficient in figure 3 and Mach number in figure 4. The lift curves for the four configurations (B_1, B_2, B_3, and B_4) were generally nonlinear at all Mach numbers of the test with increasing lift-curve slope for increasing lift coefficients (fig. 3). The alternate sweep configuration (B_3) had the lowest C_{L_α} at most Mach numbers (fig. 4) due to the higher leading-edge sweep. There was little difference in C_{L_α} for the remaining three configurations with the alternate fatness ratio body (B_2) having slightly the higher C_{L_α} at the transonic and supersonic speeds. Also, the configuration with the alternate forebody length ratio (B_4) did not have as great an increase in C_{L_α} near Mach 1 as the other bodies.

With exception of the highest Mach number of the test, B_2 had the lowest C_{D_0} of all configurations (fig. 4), which can be attributed to the lower ratio of drag-producing frontal area to lift-producing planform area (S_π/S). Configuration B_3 had the next lower value of C_{D_0}, with the remaining two bodies having higher but essentially equal values of this parameter. At all Mach numbers, configuration B_3 had the highest drag due to lift (fig. 3). The remaining three configurations all had similar values of drag due to lift, except at Mach number 10.6, where B_2 had a somewhat lower value than the others.

With exception of Mach number 0.65, configuration B_2 had by far the greater $(L/D)_{max}$ of the four configurations (fig. 4), thus indicating that reducing the fatness ratio S_π/S is effective in increasing aerodynamic efficiency. This effect can be attributed primarily to the lower C_{D_0} at most Mach numbers and the lower drag due to lift at Mach number 10.6 for the B_2 configuration. It also appears that, with exception of the lowest subsonic Mach numbers, changes in sweep angle and forebody length ratio from the nominal configuration had only minor effects on $(L/D)_{max}$ (fig. 4). For configuration B_2 at the hypersonic speeds, values of $(L/D)_{max}$ varied from about 5.4 at Mach number 5 to about 4.1 at Mach number 10.

For most Mach numbers below about 2, the pitching-moment curves were reasonably linear (fig. 3). All four configurations exhibited positive longitudinal stability near $(L/D)_{max}$ for the selected moment reference centers, with configuration B_2 having the greater level of stability at all Mach numbers of the test (fig. 3). As shown in figure 4, the aerodynamic centers moved forward with increasing supersonic Mach numbers as expected, and for B_1 and B_2, gradually moved rearward at the higher hypersonic speeds. The overall travel from the most aft to the most forward locations varied from about 11 percent $\bar{c}$ for B_4 to about 23 percent $\bar{c}$ for B_2.

As previously indicated, the sting support exited from the aft-upper surface of the models to provide an undisturbed lower body surface for testing at hypersonic speeds. This sting arrangement tended to produce a region of higher pressure on the aft-upper surface than would be obtained without the sting, resulting in a slight negative C_{L_0} and a small positive C_{m_0} at the lower speeds as can be seen in figure 3 for all the configurations. As anticipated, this effect essentially disappeared at the hypersonic Mach numbers of the test.

Lateral-directional characteristics– The lateral-directional aerodynamic characteristics of the nominal (B_1) and alternate sweep (B_3) configurations are presented in figure 5 for an angle of attack of approximately 5°. The difference in angle of attack between the two configurations is due to the fact that the sting exited from each of the models at a slightly different angle. Both configurations had negative directional stability ($-C_{n_\beta}$) at Mach numbers below about 2, but had essentially neutral stability above this speed. Of the two configurations, B_3 tended toward the greater negative value of directional stability in all cases. The configurations both had nearly equal and positive values of effective dihedral ($-C_{l_\beta}$) at all Mach numbers of the test. Both configurations had essentially zero side-force coefficients at all angles of sideslip for the subsonic Mach numbers, but at higher speeds, C_Y became negative for positive values of β.

It is interesting to note that the two configurations had essentially neutral directional stability and positive effective dihedral at the higher speeds, possibly indicating that relatively small vertical tails would be required.

Complete Body With Wings

The effects of adding thin wings, or strakes, to the alternate sweep configuration (B_3) are presented in figures 6 and 7. The longitudinal aerodynamic characteristics are presented as a function of lift coefficient (fig. 6) and summarized as a function of Mach number (fig. 7). For comparison, the results of configuration B_2 (from fig. 4) also are shown in figure 7. At all Mach numbers, adding wings to B_3 increased the lift-curve slope, resulting in a higher value of lift coefficient for a given positive angle of attack (fig. 6). As can be seen in figure 7, the C_{L_α} of B_3W was essentially equal to that of B_2 at most Mach numbers, but at the higher hypersonic speeds, B_3W had a slightly greater value.

Except for the lowest Mach numbers of the test, adding wings to B_3 tended to lower the C_{D_0} due to the increased reference area (fig. 7). In comparison to B_2, the B_3W configuration had a higher C_{D_0} in the transonic and supersonic regimes, but had a slightly lower value at the highest Mach numbers of the test (fig. 7). Adding wings tended to reduce the drag due to lift of the B_3 configuration at all test Mach numbers (fig. 6).

As shown in figure 7, the addition of wings to B_3 increased the $(L/D)_{max}$ at all but the lowest Mach number of the test. This effect is due to the lower C_{D_0}, lower drag due to lift, and higher C_{L_α} of the B_3W configuration in comparison to B_3. Comparing configurations B_3W and B_2 (fig. 7), it can be seen that in the supersonic range, B_2 had a slightly higher $(L/D)_{max}$ due primarily to its lower C_{D_0}. However, at the higher speeds, B_3W had a greater $(L/D)_{max}$ than B_2 because of its slightly higher C_{L_α} and slightly lower C_{D_0} (fig. 7). At the hypersonic speeds, $(L/D)_{max}$ of the B_3W configuration ranged from about 5.3 at Mach number 5 to about 4.9 at Mach number 10.

Adding wings to configuration B_3 had little effect on the longitudinal stability at subsonic and supersonic speeds, but tended to increase stability at the hypersonic Mach numbers (fig. 6). The aerodynamic centers near $(L/D)_{max}$ were somewhat more rearward on the B_3W configuration in comparison to B_3 for Mach numbers from about 3 to 10. Also, except for Mach numbers from about 4 to 8, the aerodynamic centers of B_3W were forward of those for B_2 (fig. 7).

Forebodies

Longitudinal characteristics– The longitudinal aerodynamic characteristics of the forebodies of the nominal (B_5) and alternate sweep (B_6) configurations are presented as a function of lift coefficient (fig. 8) and Mach number (fig. 9). During the tests, $(L/D)_{max}$ was not reached at Mach numbers below 5, and therefore for these speeds, the values of $(L/D)_{max}$ and aerodynamic center are not summarized in figure 9. The data shown in figures 8 and 9 have not been adjusted for the base drag of the forebodies.

At all Mach numbers, the lift-curve slope of the B_6 configuration was lower than that of B_5 due to the higher leading-edge sweep of B_6. The B_6 configuration had a lower C_{D_0} but a higher drag due to lift than the B_5 forebody at all Mach numbers (figs. 8 and 9). These results are consistent with those of the complete configurations (B_1 and B_3) previously discussed. However, at the higher hypersonic speeds, the $(L/D)_{max}$ of the B_6 configuration was higher than that of B_5 (fig. 9) by a greater increment than B_3 compared to B_1 (fig. 4). There were little or no differences in the longitudinal stability between B_5 and B_6 (fig. 8), and the aerodynamic centers near $(L/D)_{max}$ at the hypersonic speeds were essentially identical (fig. 9). The aerodynamic centers of the forebodies (B_5 and B_6) were farther aft (fig. 9) than those of the complete configurations (fig. 4).

Lateral-directional characteristics– The lateral-directional aerodynamic characteristics of the forebody (B_5) of the nominal configuration are presented in figure 10 for several Mach numbers at zero angle of attack. The three parameters C_n, C_l, and C_Y were all essentially linear with angle of sideslip for the Mach numbers considered in the test. The B_5 configuration had positive directional stability (C_{n_β}) at all Mach numbers with the greater level at Mach number 7.38. In all cases, the effective dihedral (C_{l_β}) was essentially zero and the side-force coefficients were negative at positive angles of sideslip.

Volume/Planform Parameter

The results from the previous sections are shown summarized (circular symbols) in figure 11 for Mach number 6.8 in terms of $(L/D)_{max}$ as a function of the volume parameter ($V^{2/3}/S$), which exerts a large influence on maximum lift-drag-ratio characteristics. For cruise vehicles, this volume parameter will probably range from about 0.14 to 0.24. The data on this figure are for laminar boundary layers, and the Reynolds numbers (R_l) are based on body length. The Reynolds numbers for the present data are summarized below:

Configuration	$R_l \times 10^{-6}$
B_1	4.0
B_2	4.5
B_3	4.6
B_4	4.1
B_3W	4.6
B_5	2.6
B_6	3.0
B_1HV	4.0

The trends of the present data are consistent with the experimental values of $(L/D)_{max}$ for a number of idealized shapes from reference 11, which are presented for comparison. Configurations B_2 and B_3W had the highest values of $(L/D)_{max}$ of the present configurations as a result of their greater planform or lifting area in comparison to their volumes. It should be noted that the values of $(L/D)_{max}$ for the two forebodies (B_5 and B_6) have not been adjusted for base drag as have the results from reference 11. It is estimated that this adjustment would increase the $(L/D)_{max}$ by about 0.3 and 0.4 for the B_5 and B_6 configurations, respectively.

The addition of horizontal tails (H) and vertical tails (V) to the B_1 configuration (ref. 10) resulted in an $(L/D)_{max}$ value of about 3.8 as indicated by the square symbol in figure 11. The reduction in the volume/planform parameter was a result of the added plan area of the horizontal tails, which overshadowed the small increase in volume due to the stabilizing surfaces. Thus, it is obvious that the aerodynamic efficiency of this all-body concept (B_1HV) could be improved by shaping the body toward the B_2 configuration.

The triangular symbol in figure 11 shows the experimental value of $(L/D)_{max}$ obtained for a wing-body configuration in reference 5. In comparison with the B_1HV configuration, the wing-body concept had a slight advantage in aerodynamic efficiency at this Mach number, although these results do not include trim penalties.

SUMMARY OF RESULTS

An experimental investigation to determine the effects of several variations in body shape on the aerodynamic characteristics of an all-body hypersonic aircraft configuration was conducted at Mach numbers from 0.65 to 10.61. Some of the most pertinent results are as follows:

1. Of the four complete bodies (forebody plus afterbody), the configuration with the lowest ratio of cross-sectional to body planform area had the highest maximum lift-drag ratio $(L/D)_{max}$ at all but the lowest Mach number of the test. For this configuration at hypersonic speeds, the values of $(L/D)_{max}$ varied from about 5.4 at Mach number 5 to about 4.1 at Mach number 10.

2. With exception of the lowest subsonic Mach numbers, an increase in body sweep angle or in forebody length ratio had only minor effects on $(L/D)_{max}$.

3. For the selected moment reference centers, all configurations had positive longitudinal stability near $(L/D)_{max}$ at most Mach numbers of the test. Of the four complete bodies, the configuration with the lowest ratio of cross-sectional to body planform area had the greater level of longitudinal stability at all Mach numbers of the test.

4. For the complete bodies, the overall travel of the aerodynamic centers with Mach number from the most aft to the most forward location varied from about 11 to 23 percent of the mean aerodynamic chord depending on the configuration.

5. At the higher speeds, the complete bodies with the nominal and higher sweep had essentially neutral directional stability and positive effective dihedral.

6. Except at the lowest Mach numbers, the addition of thin wings, or strakes, to the higher sweep body increased the $(L/D)_{max}$. At hypersonic speeds, the $(L/D)_{max}$ of this winged configuration varied from about 5.3 at Mach number 5 to about 4.9 at Mach number 10.

7. The addition of thin wings to the higher sweep body had little effect on the longitudinal stability at subsonic and supersonic speeds, but tended to increase stability at the hypersonic Mach numbers.

Ames Research Center
National Aeronautics and Space Administration
Moffett Field, Calif., 94035, January 27, 1972

REFERENCES

1. Gregory, Thomas J.; Petersen, Richard H.; and Wyss, John A.: Performance Tradeoffs and Research Problems for Hypersonic Transports. J. Aircraft, vol. 2, no. 4, July-Aug. 1965, pp. 266–271. Also AIAA paper 64–605.

2. Petersen, Richard H.; Gregory, Thomas J.; and Smith, Cynthia L.: Some Comparisons of Turboramjet-Powered Hypersonic Aircraft for Cruise and Boost Missions. J. Aircraft, vol. 3, no. 5, Sept–Oct. 1966, pp. 398–405. Also AIAA Paper 65–759.

3. Nelms, Walter P., Jr.; and Axelson, John A.: Experimental and Theoretical Aerodynamic Characteristics of Representative Hypersonic Cruise Configurations. Part I, Lift and Drag; Part II, Stability and Trim. NASA TM X-1462, 1967.

4. Nelms, Walter P., Jr.; Carmichael, Ralph L.; Castellano, Charles R.: An Experimental and Theoretical Investigation of a Symmetrical and a Cambered Delta Wing Configuration at Mach Numbers From 2.0 to 10.7. NASA TN D–5272, 1969.

5. Nelms, Walter P., Jr.; and Axelson, John A.: Longitudinal Aerodynamic Characteristics of Three Representative Hypersonic Cruise Configurations at Mach Numbers From 0.65 to 10.70. NASA TM X–2113, 1970.

6. Nelms, Walter P., Jr.; and Axelson, John A.: Effects of Wing Elevation, Incidence, and Camber on the Aerodynamic Characteristics of a Representative Hypersonic Cruise Configuration at Mach Numbers From 0.65 to 10.70. NASA TN D–6049, 1970.

7. Gregory, Thomas J.; Ardema, Mark D.; Waters, Mark H.: Hypersonic Transport Preliminary Performance Estimates for an All-Body Configuration. AIAA Paper 70–1224. Presented at the AIAA 7th Annual Meeting and Technical Display, Houston, Texas, October 19–22, 1970.

8. Gregory, Thomas J.; Williams, Louis J.; and Wilcox, Darrell E.: The Airbreathing Launch Vehicle for Earth Orbit Shuttle-Performance and Operation. AIAA Paper 70–270. Presented at the AIAA Advanced Space Transportation Meeting, Cocoa Beach, Florida, Feb. 4–6, 1970.

9. Williams, Louis J.: Estimated Aerodynamics of All-Body Hypersonic Aircraft Configurations. NASA TM X–2091, 1971.

10. Nelms, Walter P., Jr.; and Thomas, Charles, L.: Aerodynamic Characteristics of an All-Body Hypersonic Aircraft Configuration at Mach Numbers From 0.65 to 10.6. NASA TN D–6577, 1971.

11. Becker, John V.: Studies of High Lift/Drag Ratio Hypersonic Configurations. Proc. 4th Cong. Intl. Council of Aero. Sci., Paris, Aug. 24–28, 1964, Robert R. Dexter, ed., Sparton Books, Inc., Washington, 1965, pp. 877–910.

TABLE 1.– MODEL GEOMETRY

[Lengths are in cm and areas are in sq cm]

	B_1	B_2	B_3	B_4	B_3W	B_5	B_6
l	48.26	55.19	55.48	49.38	55.48	32.19	37.01
l_π	32.19	36.81	37.01	37.04	37.01	32.19	37.01
S	624.00	816.26	542.87	653.30	542.87* 824.71**	277.48	241.31
S_π	58.34	51.02	50.76	61.08	50.76	58.34	50.76
a_π	8.62	9.86	6.52	9.92	6.52	8.62	6.52
b_π	2.16	1.65	2.48	1.96	2.48	2.16	2.48
Λ	75°	75°	80°	75°	80°* 75°**	75°	80°
Span	25.86	29.58	19.57	26.46	19.57* 29.73**	17.24	13.04
$\bar{c}$	32.19	36.81	37.01	32.94	37.01	21.47	24.69

*Body

**Wing

TABLE 2.– BALANCE CAVITY AXIAL–FORCE COEFFICIENT (C_{A_b})

B_1 configuration					
α \ M	0.65	0.80	0.90	1.10	1.30
−2.00	0.0002	0.0001	0.0008	0.0019	0.0013
−1.00	.0002	.0001	.0010	.0019	.0013
0	.0002	.0001	.0011	.0020	.0014
1.00	.0003	.0002	.0011	.0020	.0014
2.00	.0003	.0002	.0011	.0020	.0015
4.00	.0003	.0002	.0010	.0020	.0015
6.00	.0004	.0003	.0008	.0021	.0015
8.00	.0005	.0003	.0009	.0023	.0016
10.00	.0006	.0004	.0012	.0026	.0018
12.00	.0008	.0005	.0016	.0029	.0019
14.00	.0010	.0007	.0021	.0031	.0020
α \ M	1.60	2.00	5.37	7.38	10.61
−2.00	.0008	.0004	.0001	0	−.0002
−1.00	.0009	.0005	.0001	0	−.0002
0	.0009	.0005	.0001	0	−.0002
1.00	.0009	.0005	.0001	0	−.0002
2.00	.0010	.0006	.0001	0	−.0002
4.00	.0010	.0006	.0002	.0001	−.0002
6.00	.0010	.0007	.0002	.0001	−.0002
8.00	.0011	.0007	.0002	.0001	−.0002
10.00	.0012	.0008	.0002	.0001	−.0002
12.00	.0013	.0009	.0002	.0001	−.0003
14.00	.0014	.0009	.0002	.0001	−.0003

Note: B_5 is the forebody of B_1
B_6 is the forebody of B_3

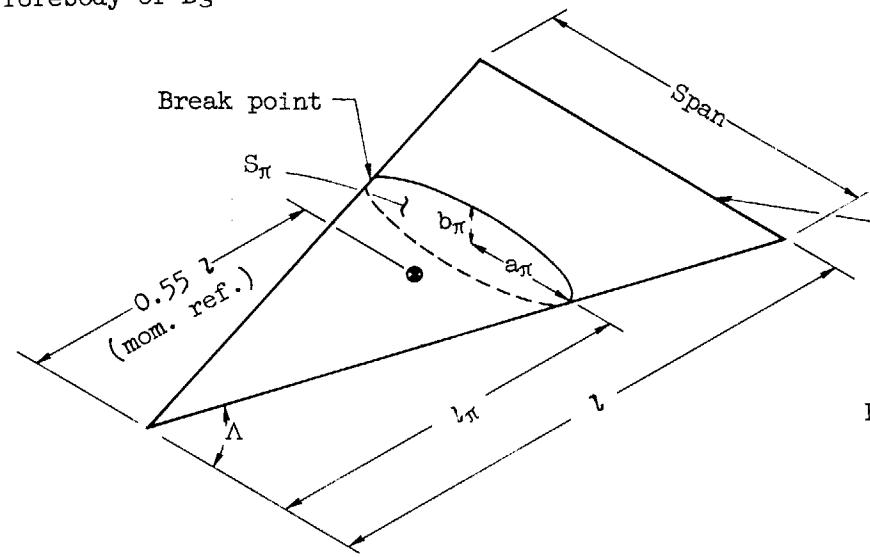

Equation for maximum cross section

$$(y/a_\pi)^2 + (z/b_\pi)^2 = 1$$

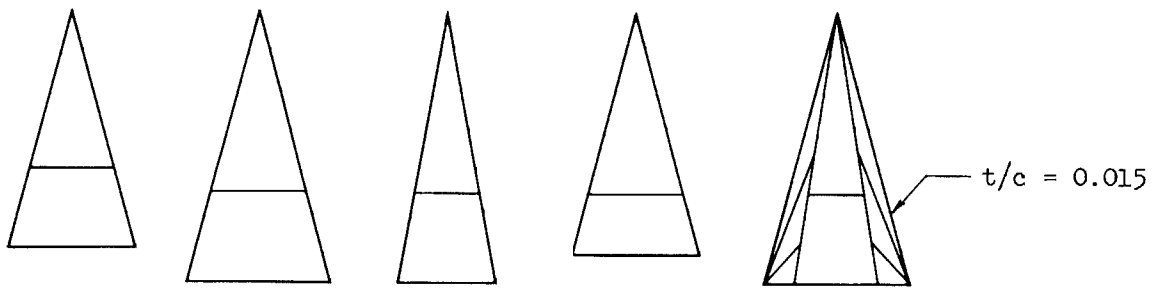

	B_1	B_2	B_3	B_4	B_3W
Λ	75°	75°	80°	75°	body 80° wing 75°
S_π/S	0.0935	0.0625	0.0935	0.0935	body 0.0935
l_π/l	0.667	0.667	0.667	0.750	0.667
a_π/b_π	4.00	5.98	2.63	5.06	2.63

Figure 1.- Model parameters.

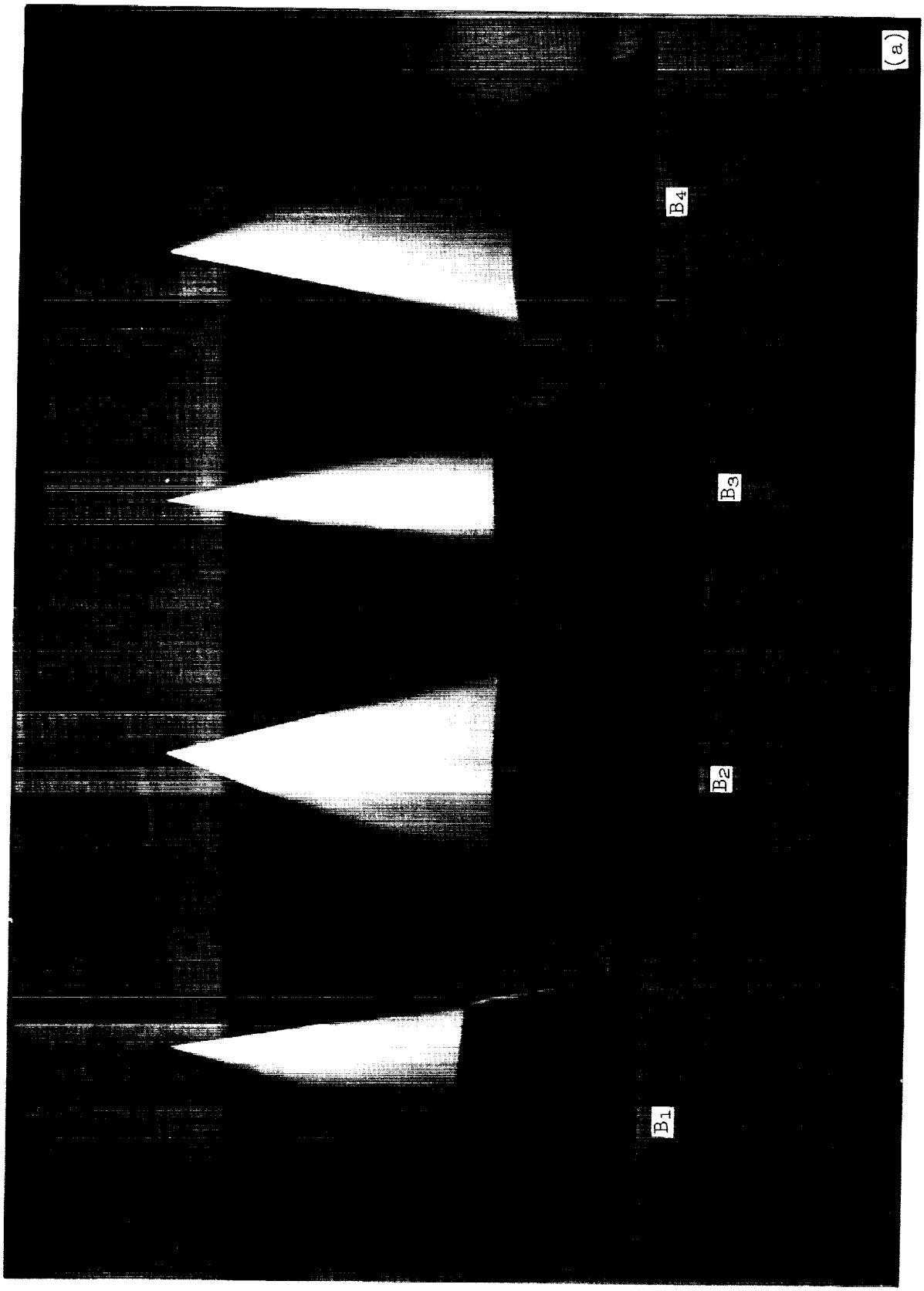

Figure 2.- Model photographs.

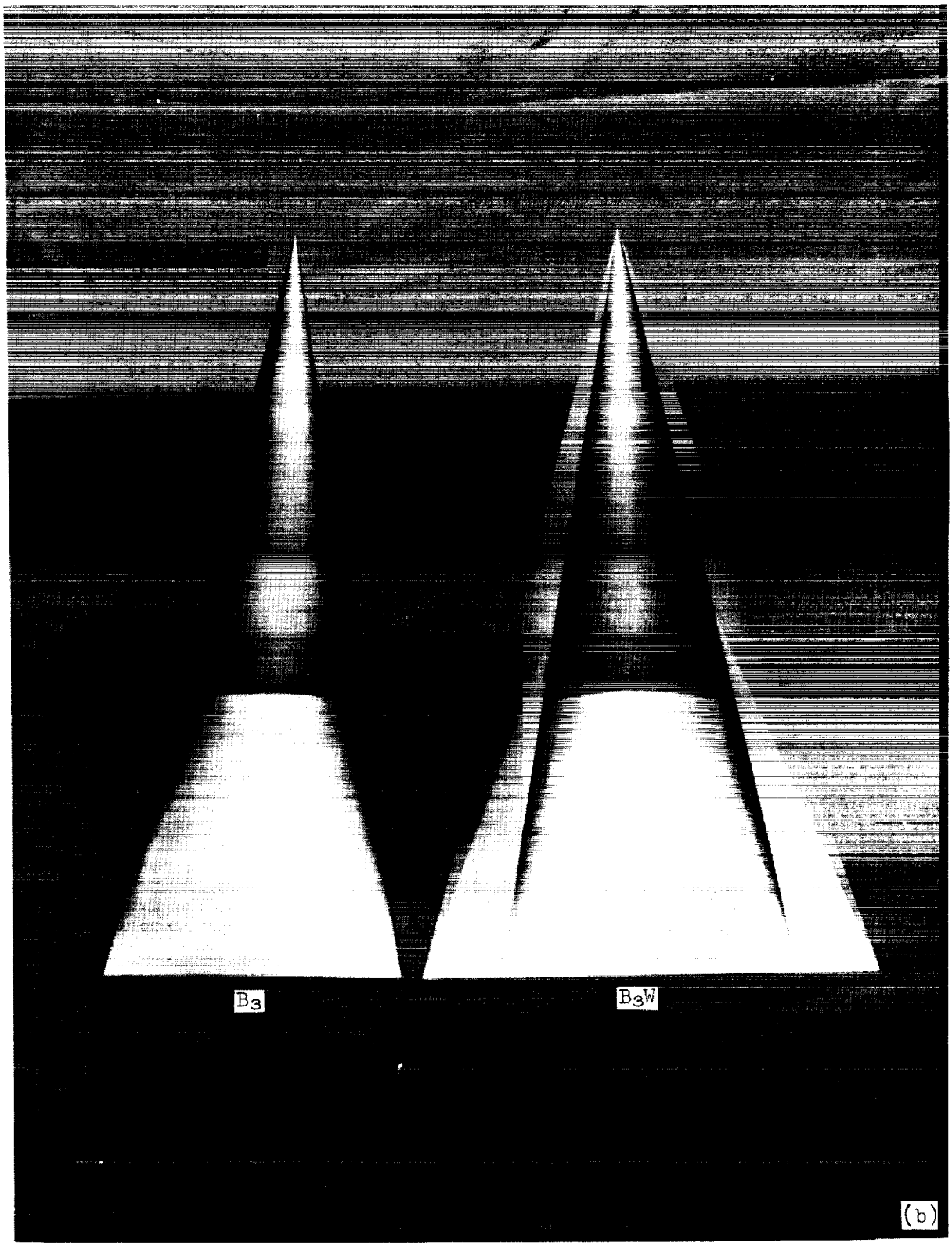

Figure 2.- Continued.

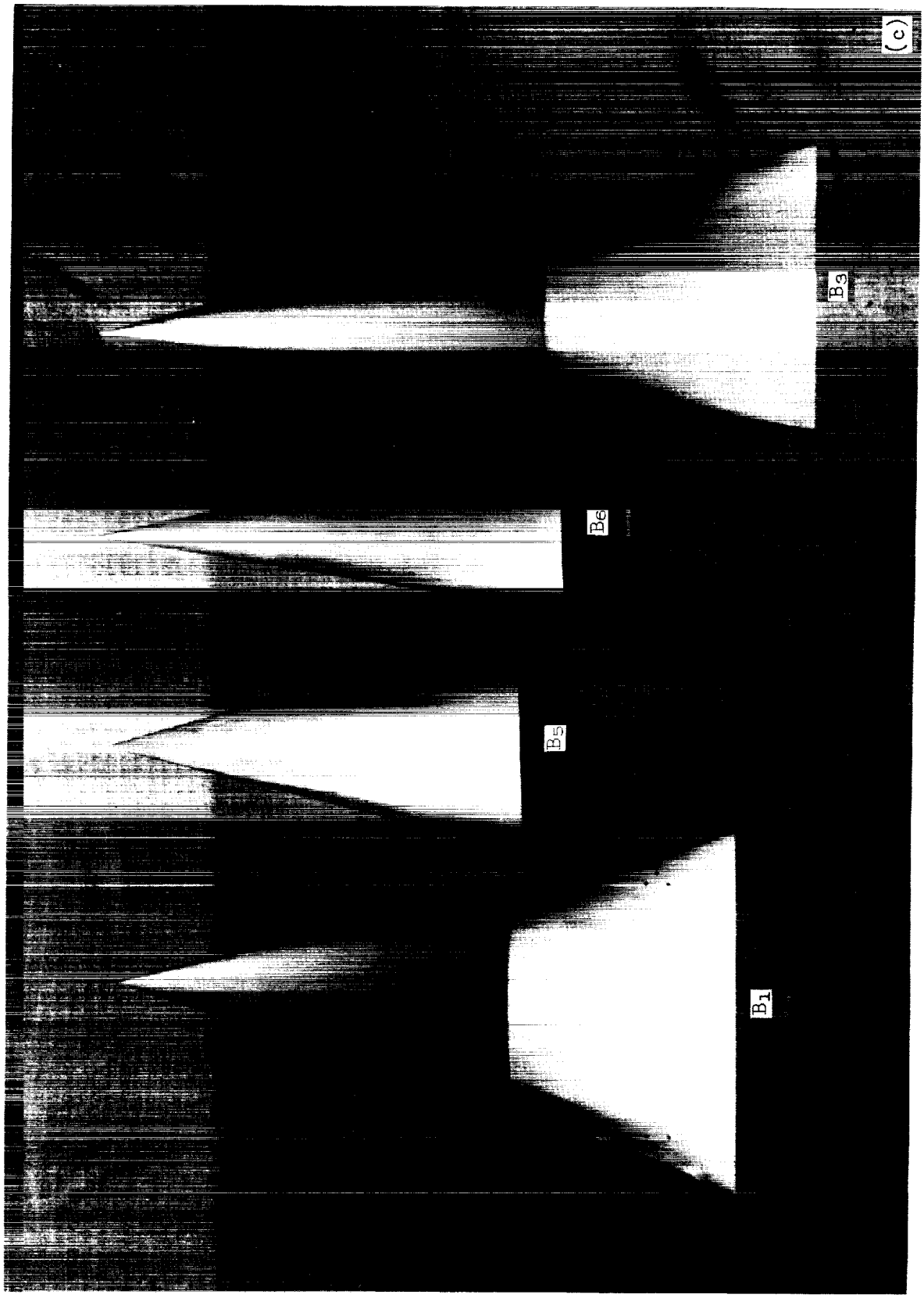

Figure 2.- Concluded.

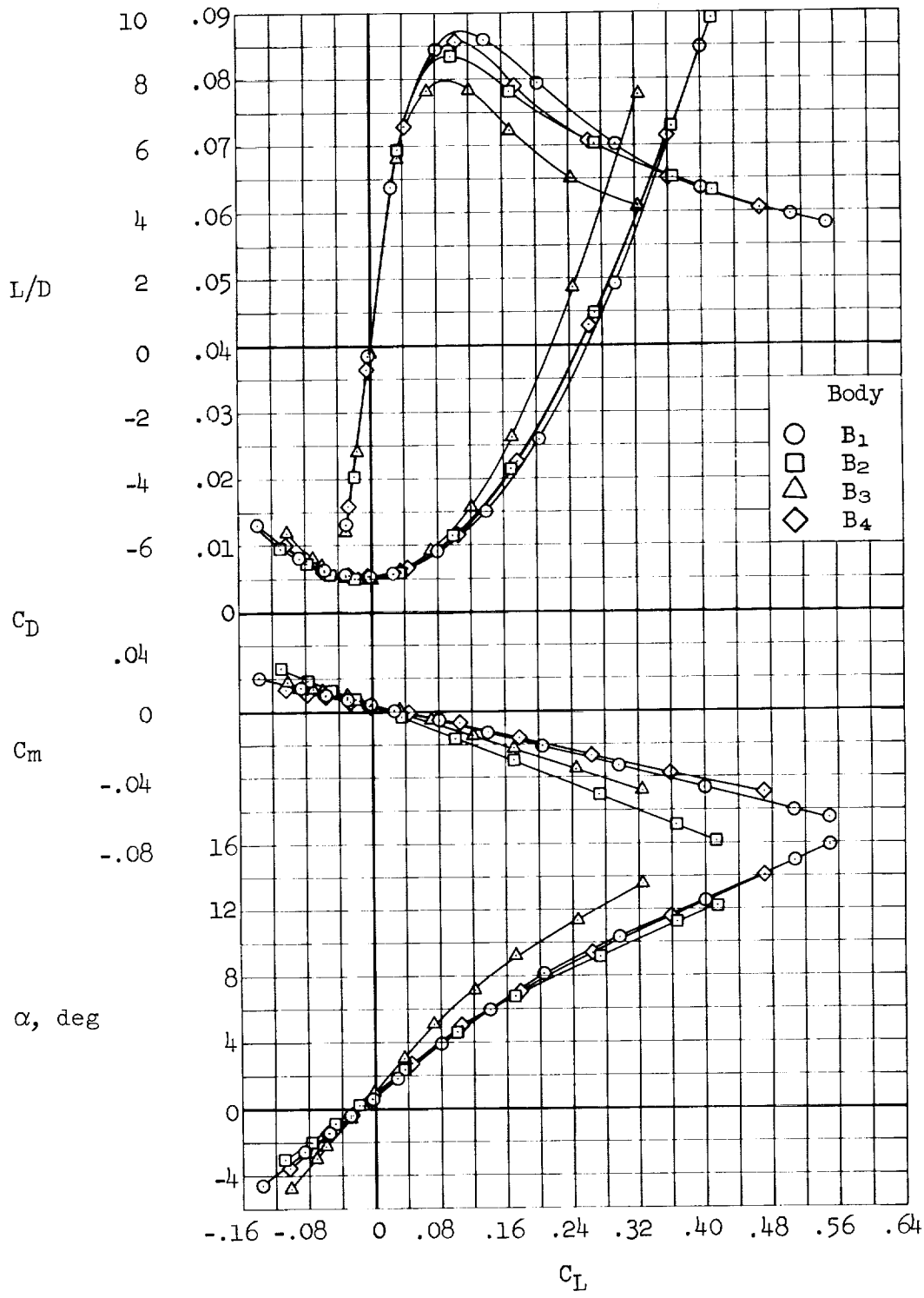

(a) M = 0.65

Figure 3.- Effect of body shape on the longitudinal aerodynamic characteristics.

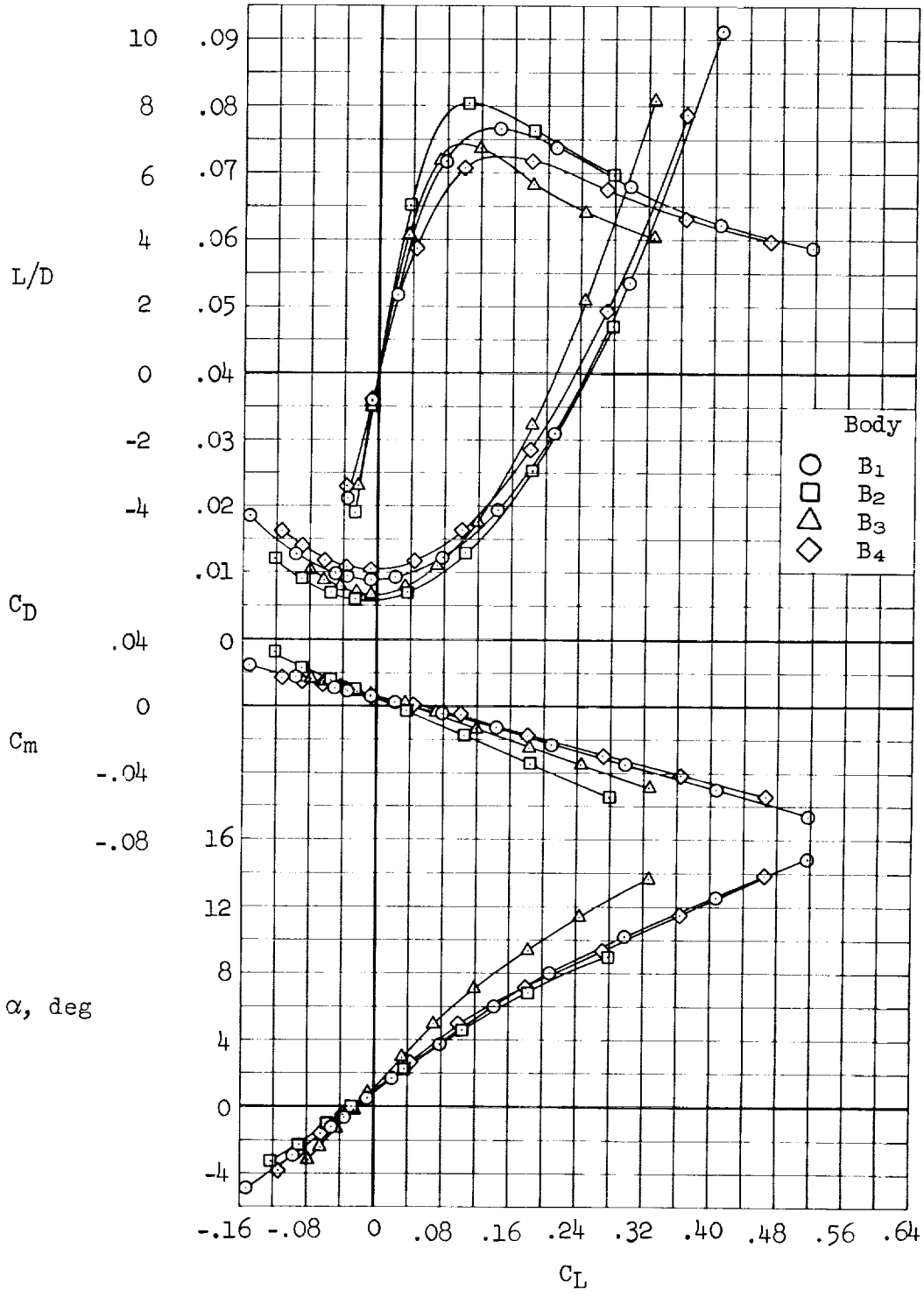

(b) M = 0.80

Figure 3.- Continued.

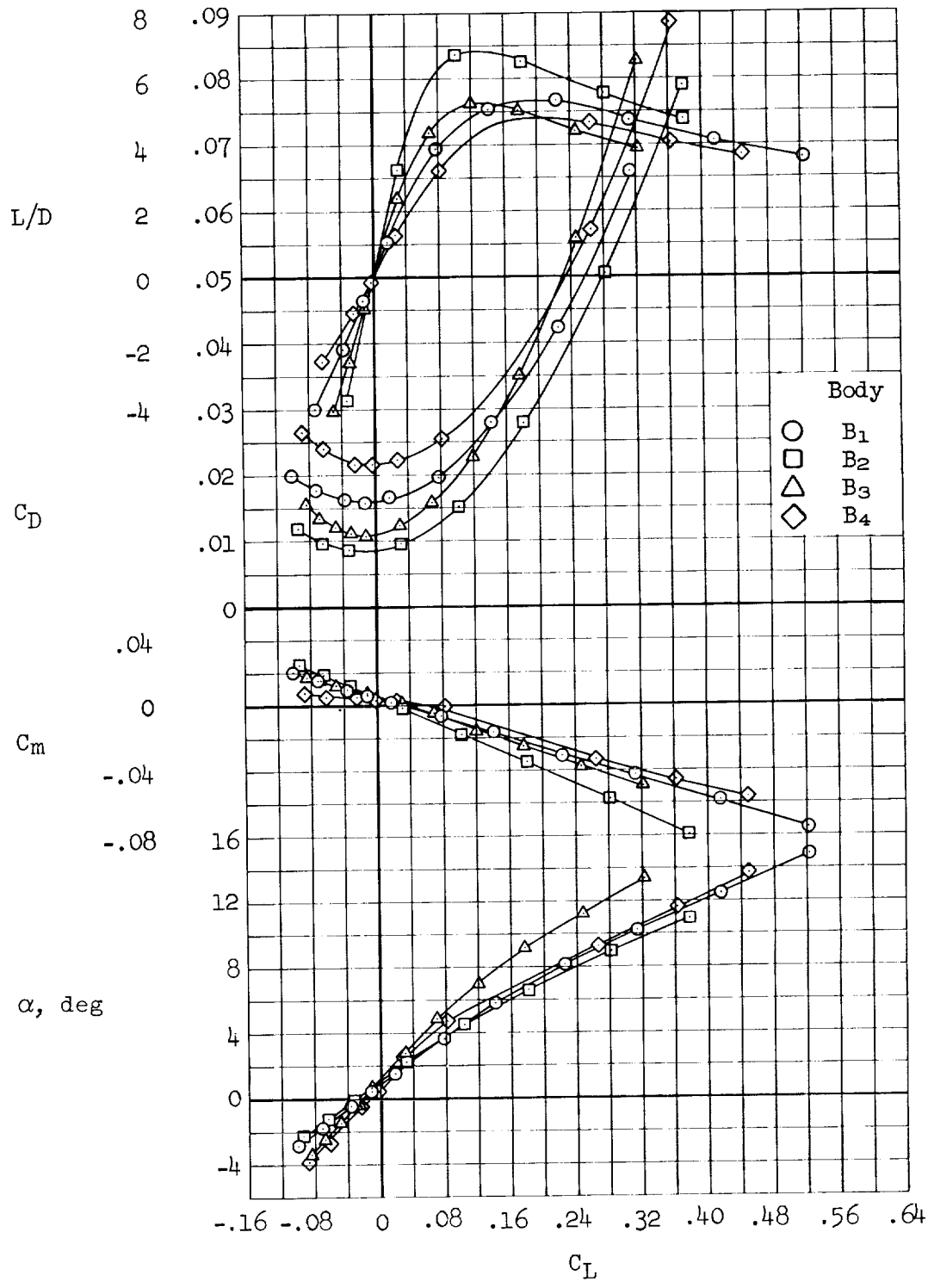

(c) M = 0.90

Figure 3.- Continued.

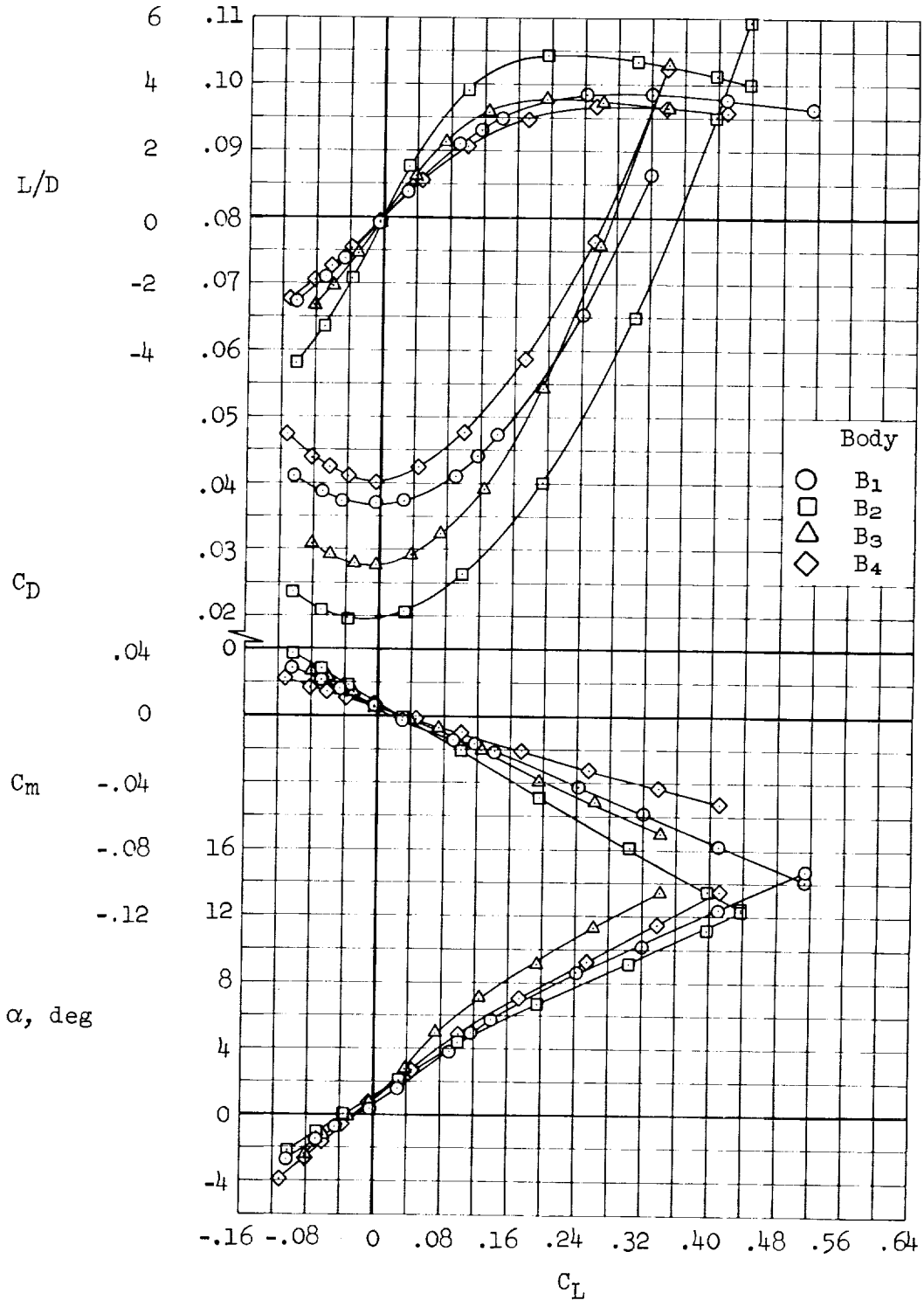

(d) M = 1.10

Figure 3.- Continued.

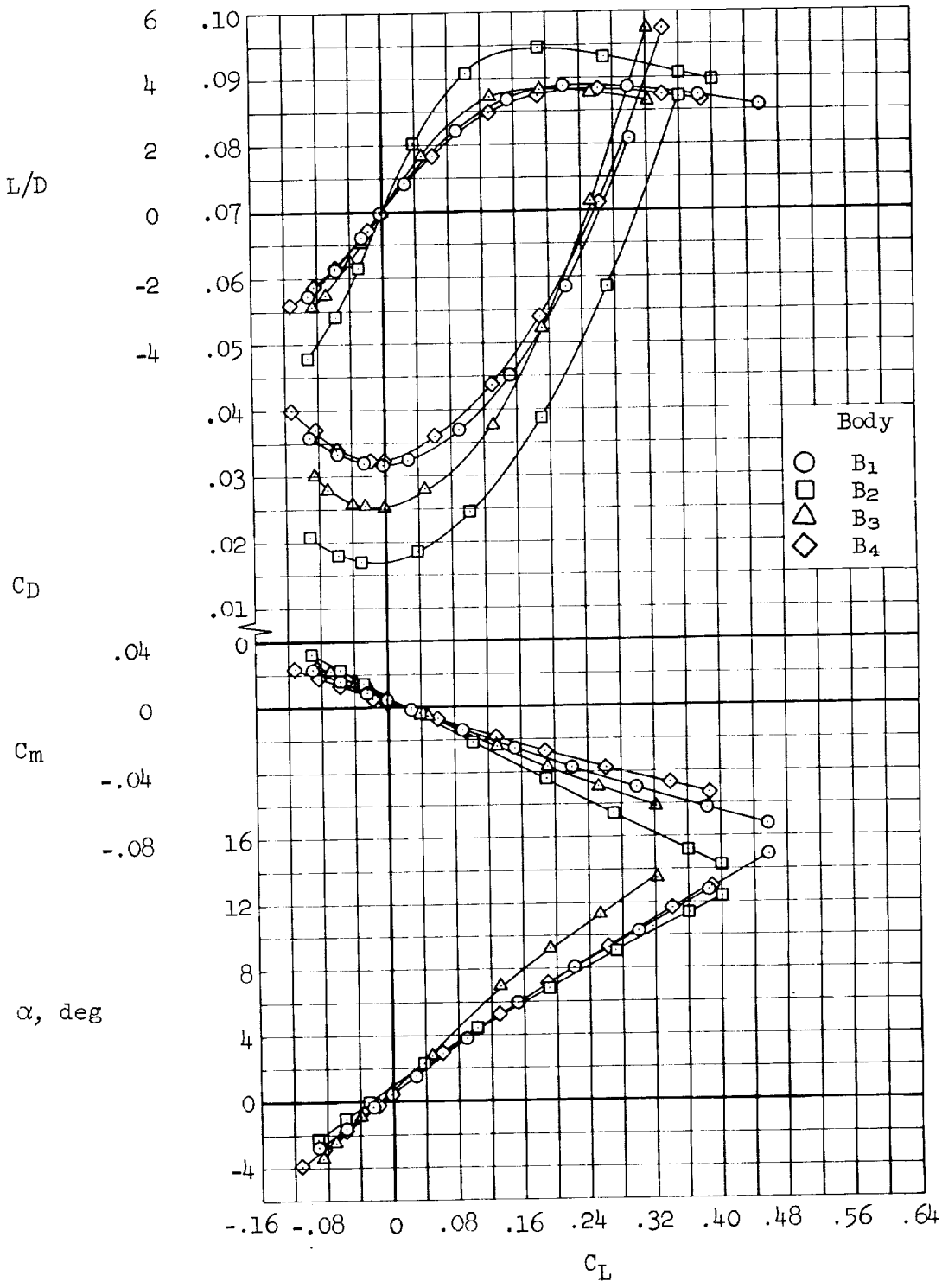

(e) M = 1.30

Figure 3.- Continued.

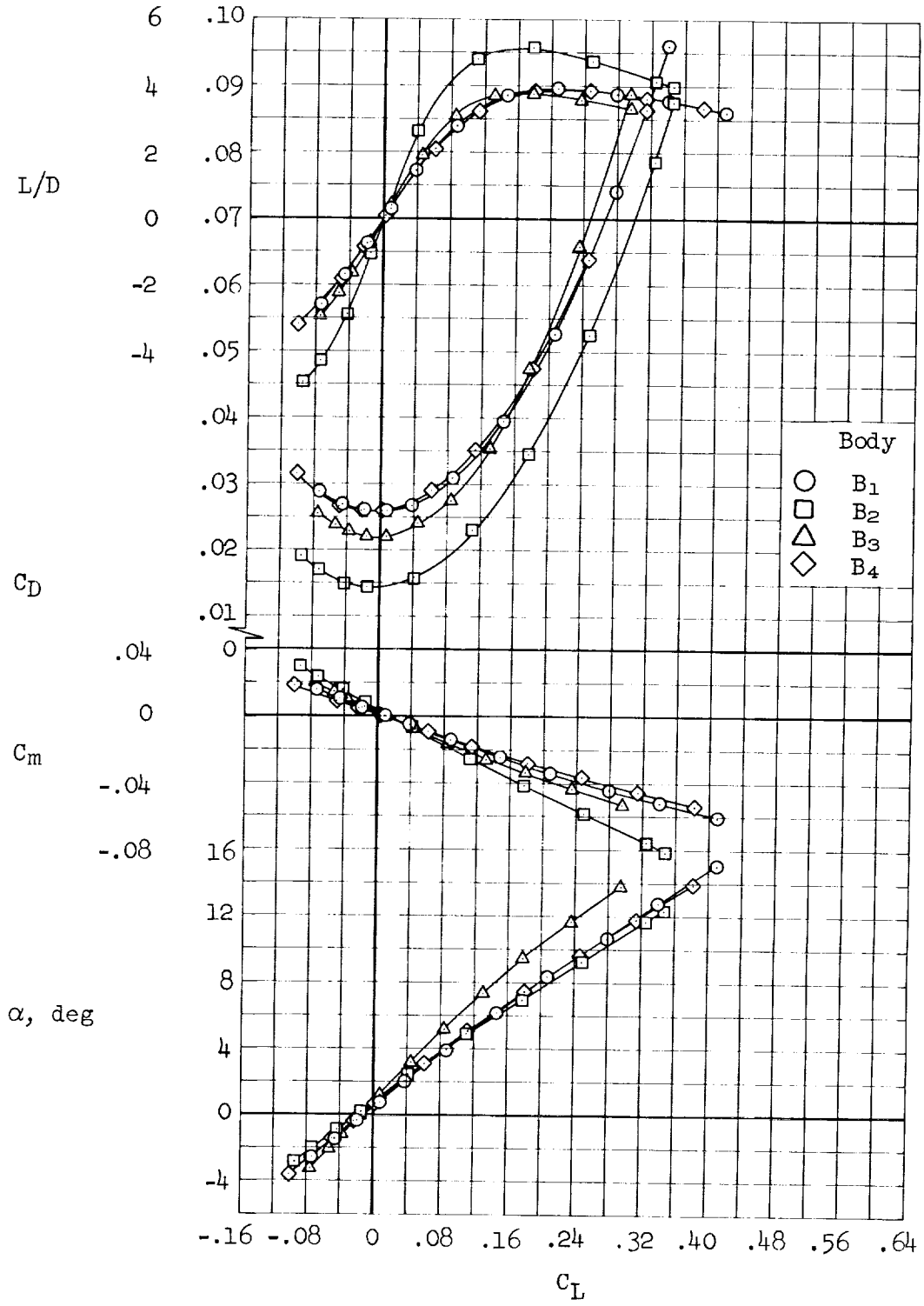

(f) M = 1.60

Figure 3.- Continued.

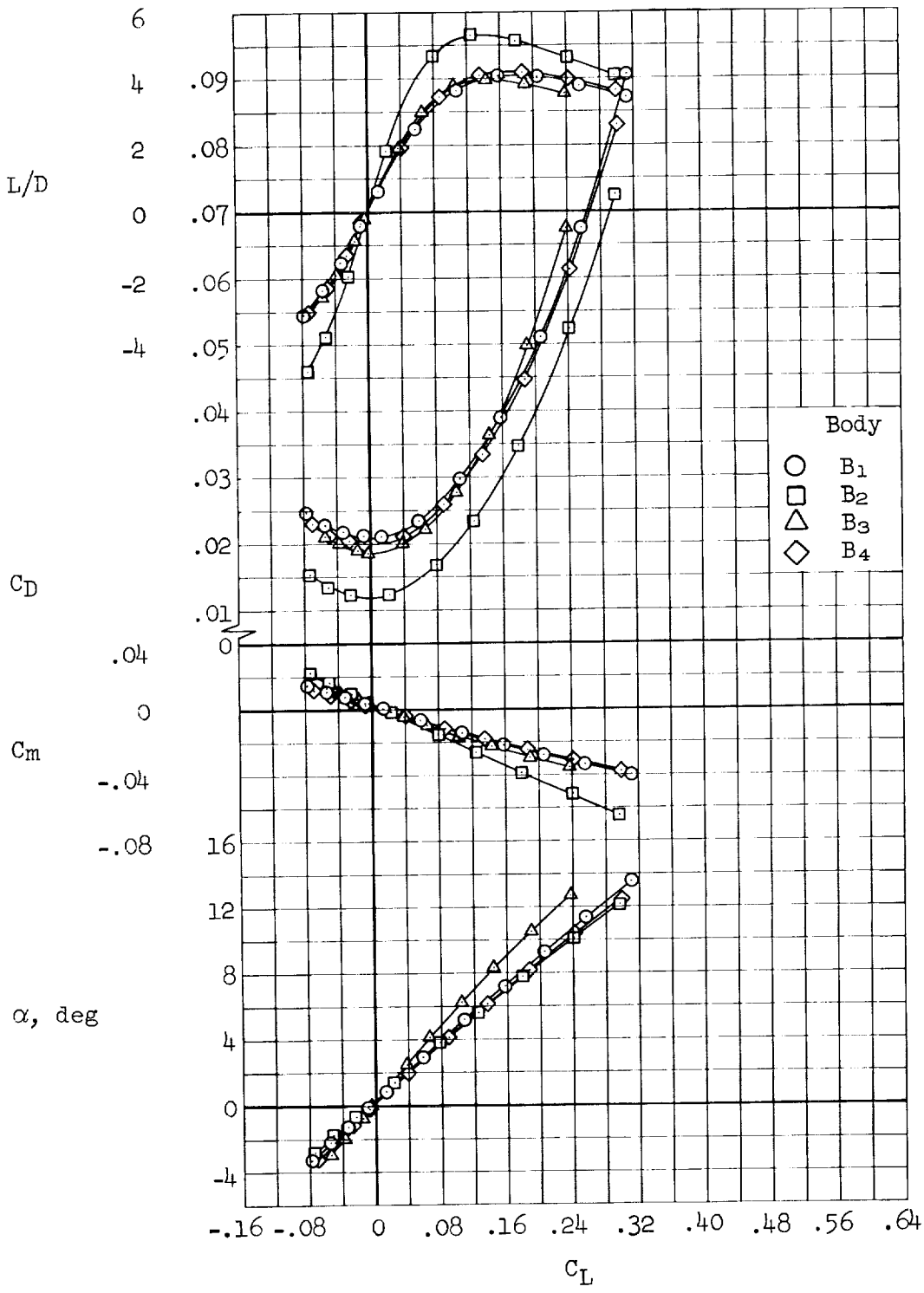

(g) M = 2.00

Figure 3.- Continued.

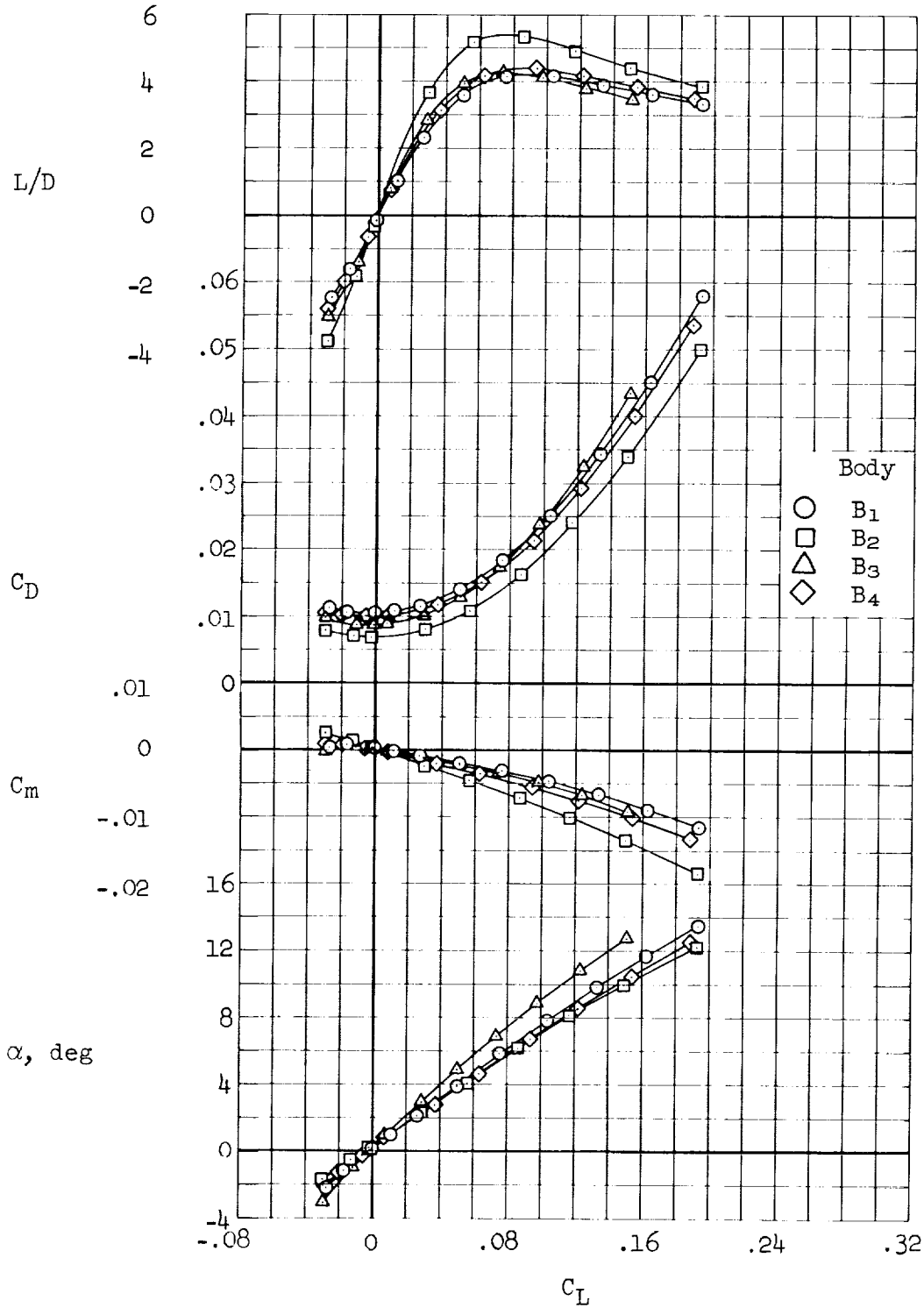

(h) M = 5.37

Figure 3.- Continued.

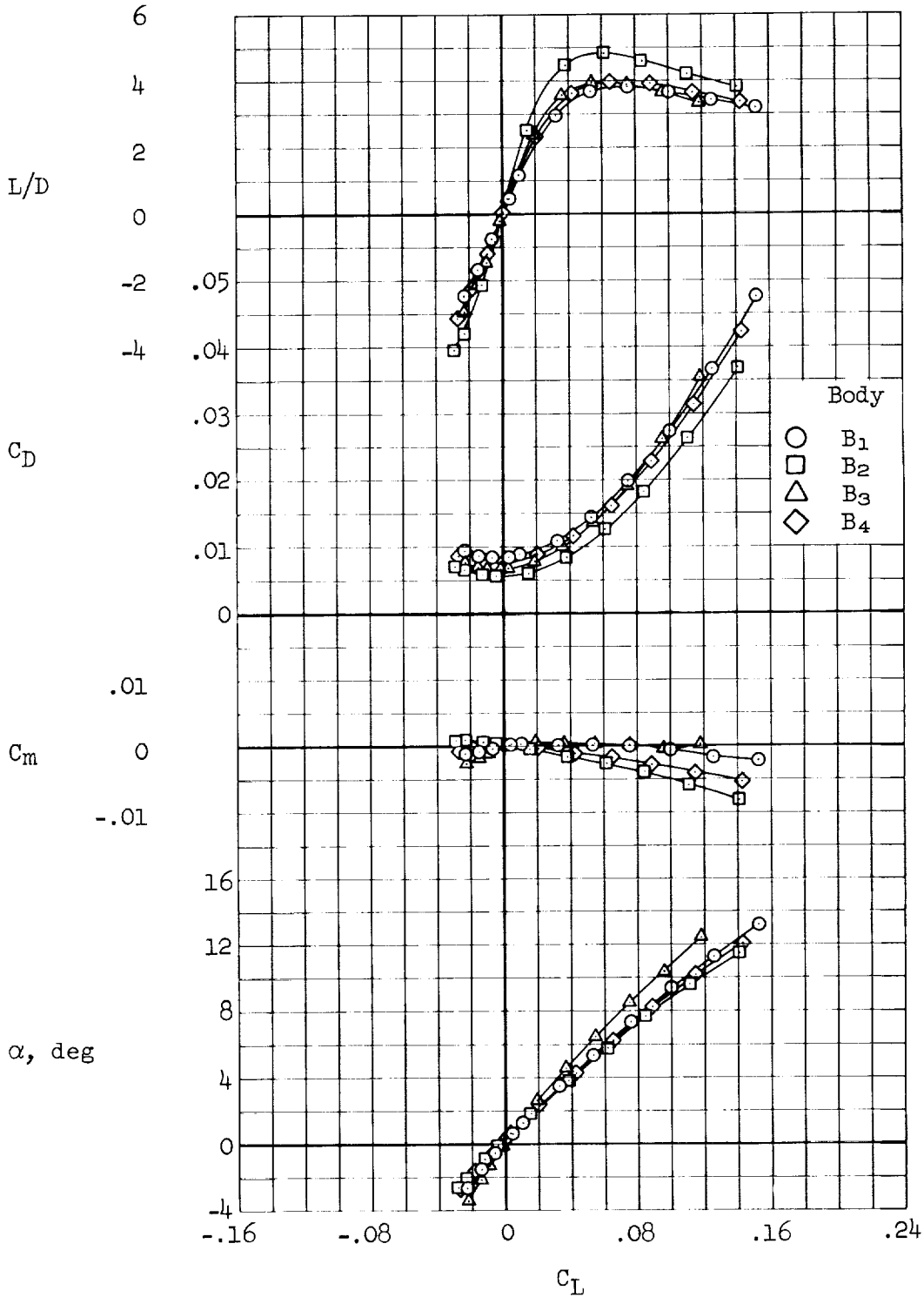

(i) M = 7.38

Figure 3.- Continued.

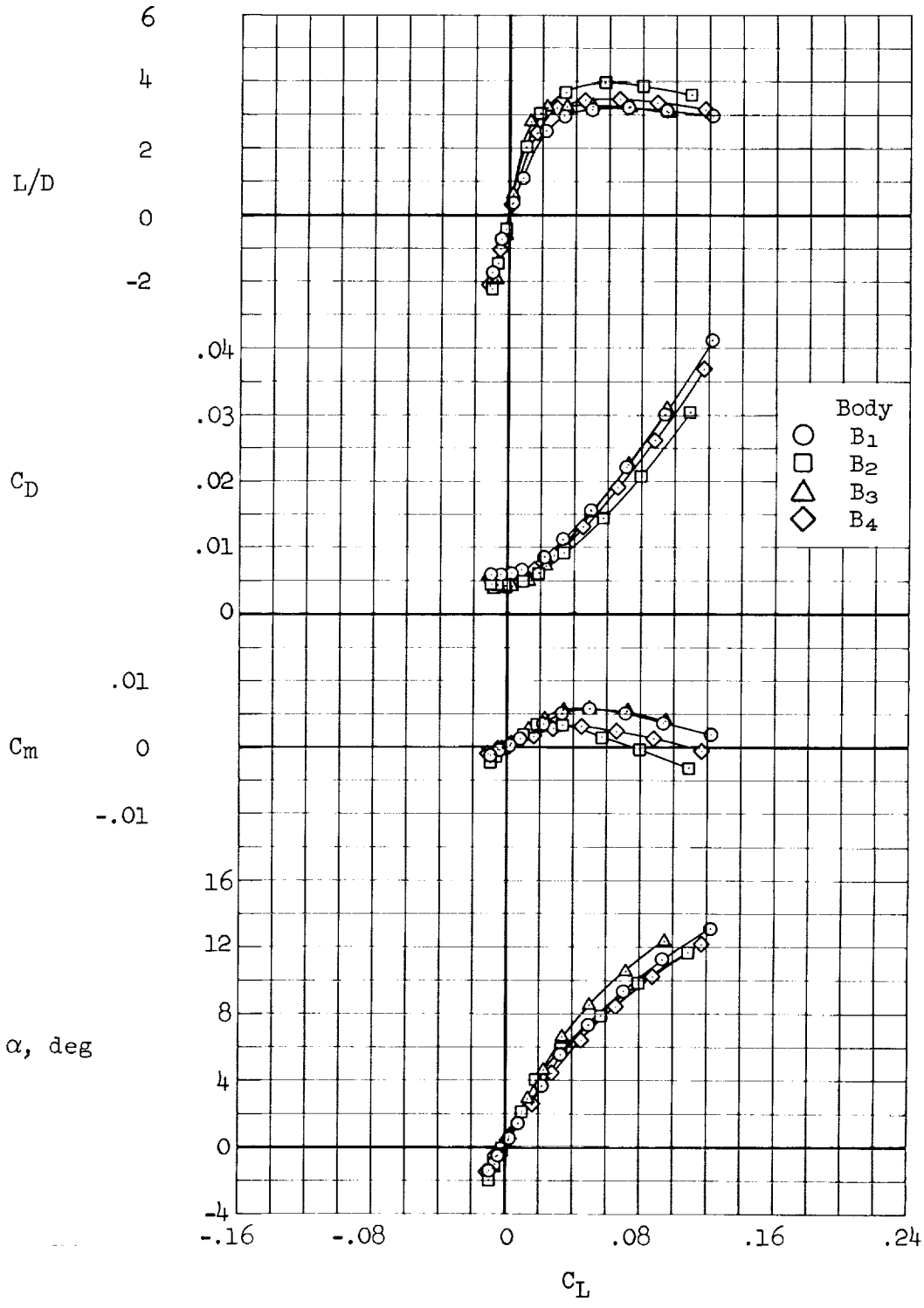

(j) M = 10.61

Figure 3.- Concluded.

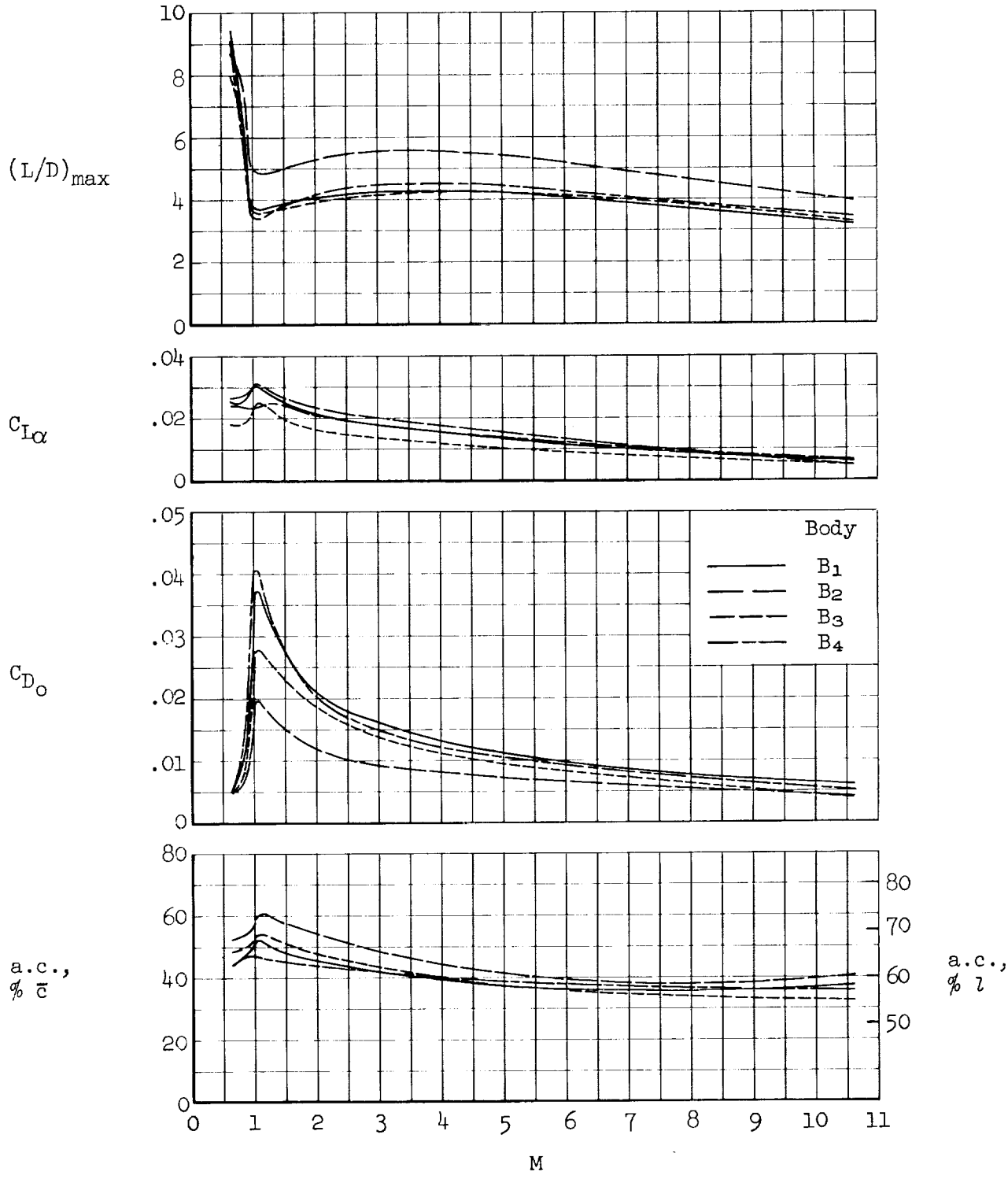

Figure 4.- Variation with Mach number of the effect of body shape on the longitudinal aerodynamic characteristics.

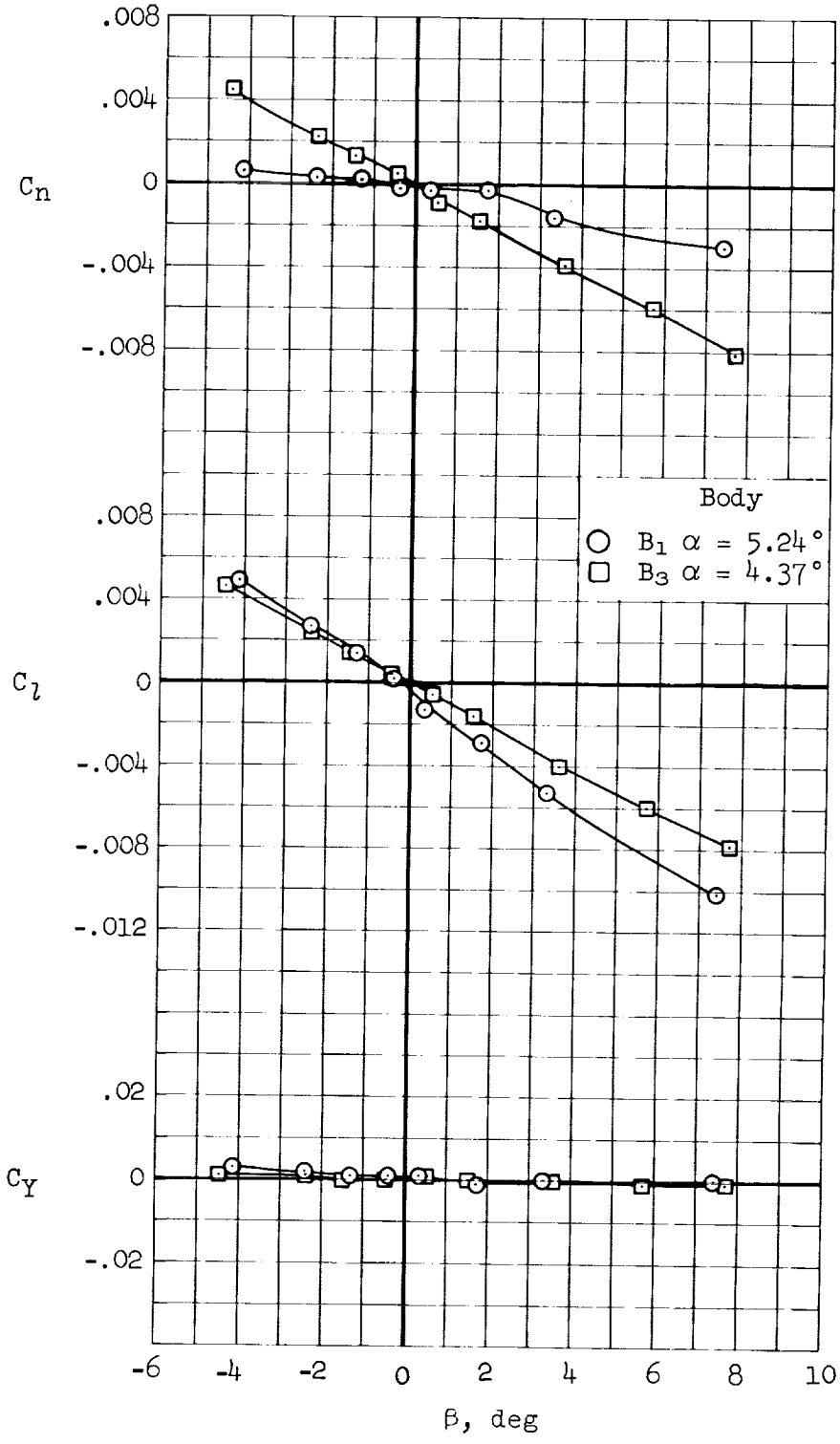

(a) M = 0.65

Figure 5.- Lateral-directional aerodynamic characteristics of the nominal and alternate sweep configurations.

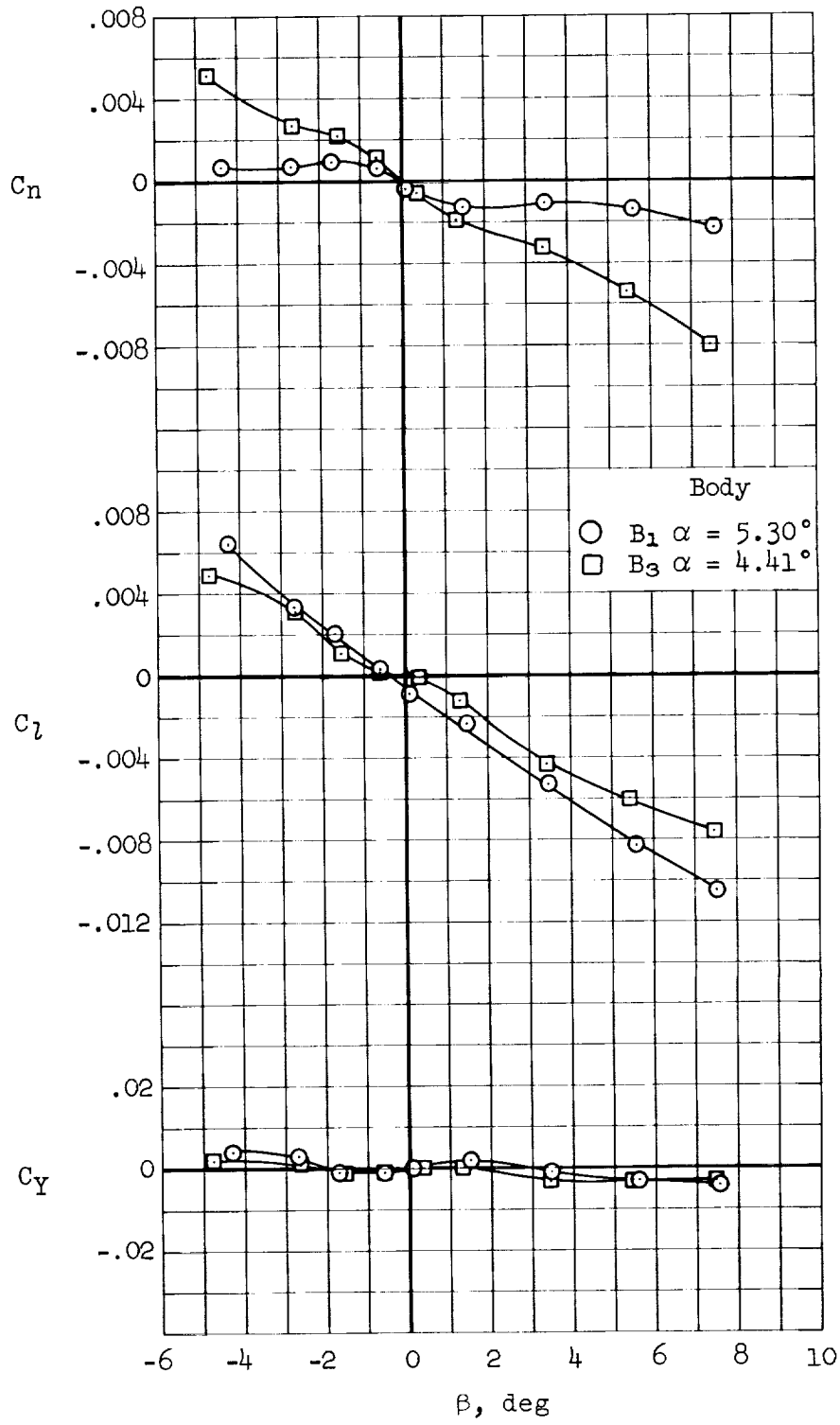

(b) M = 0.90

Figure 5.- Continued.

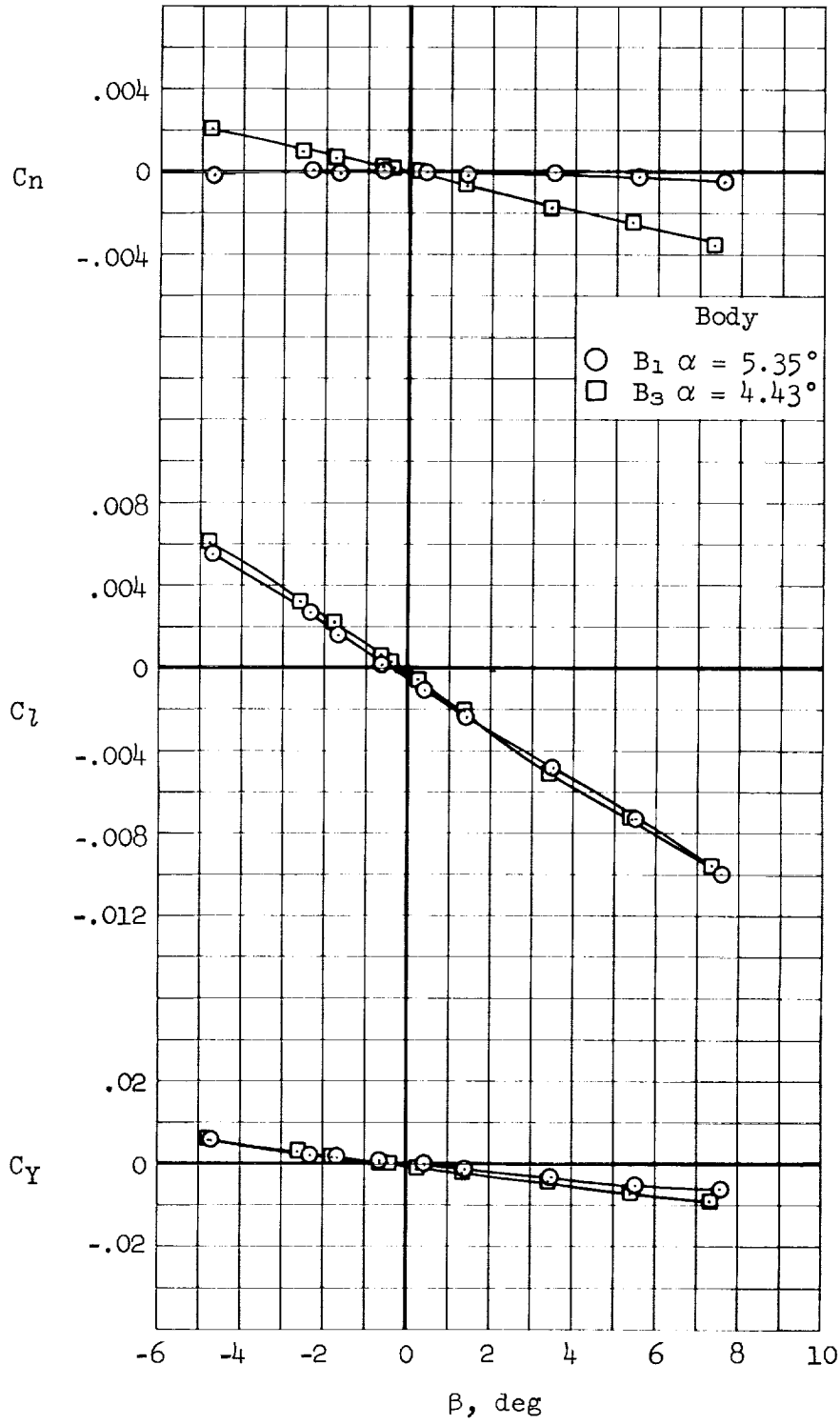

(c) M = 1.30

Figure 5.- Continued.

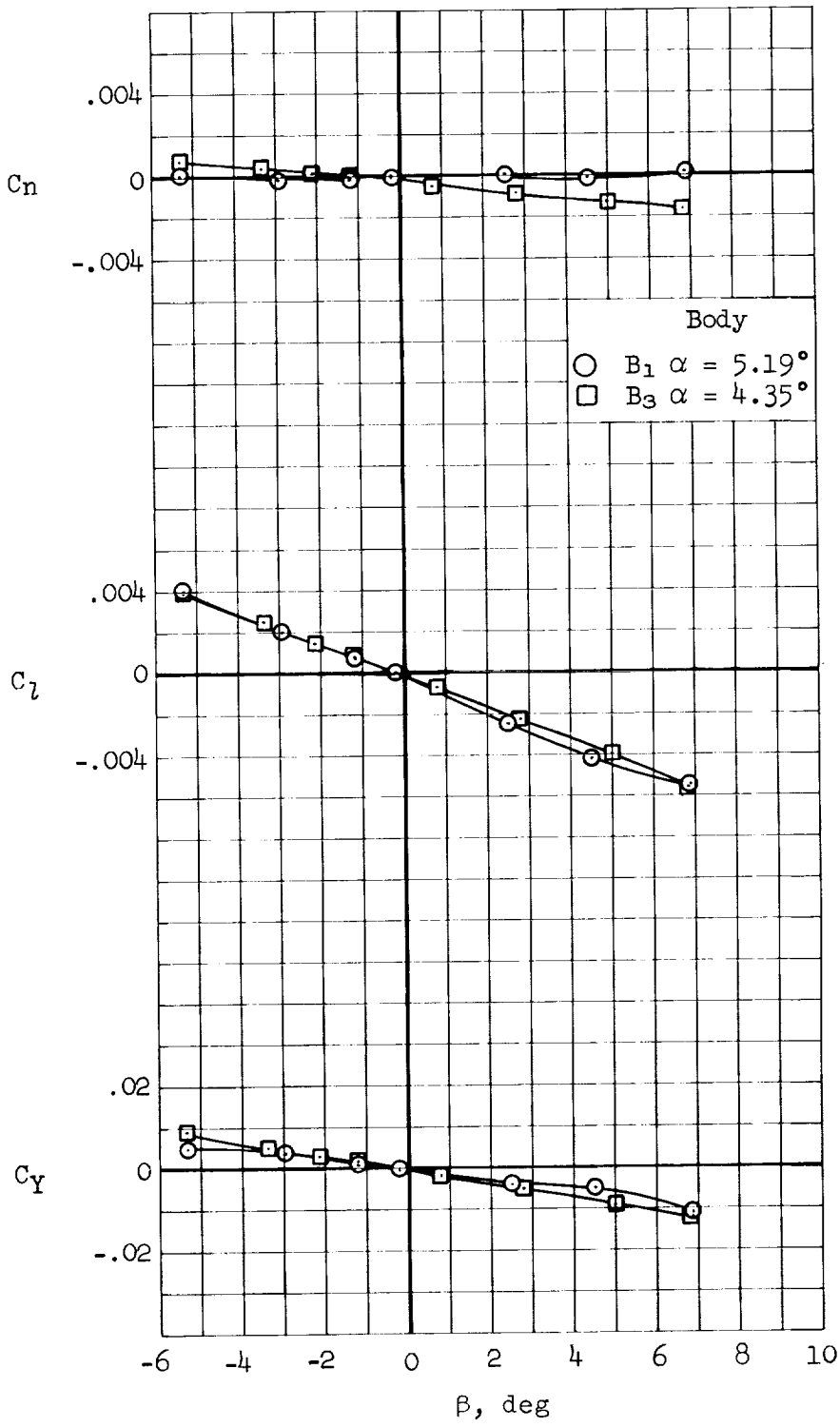

(d) M = 2.00

Figure 5.- Continued.

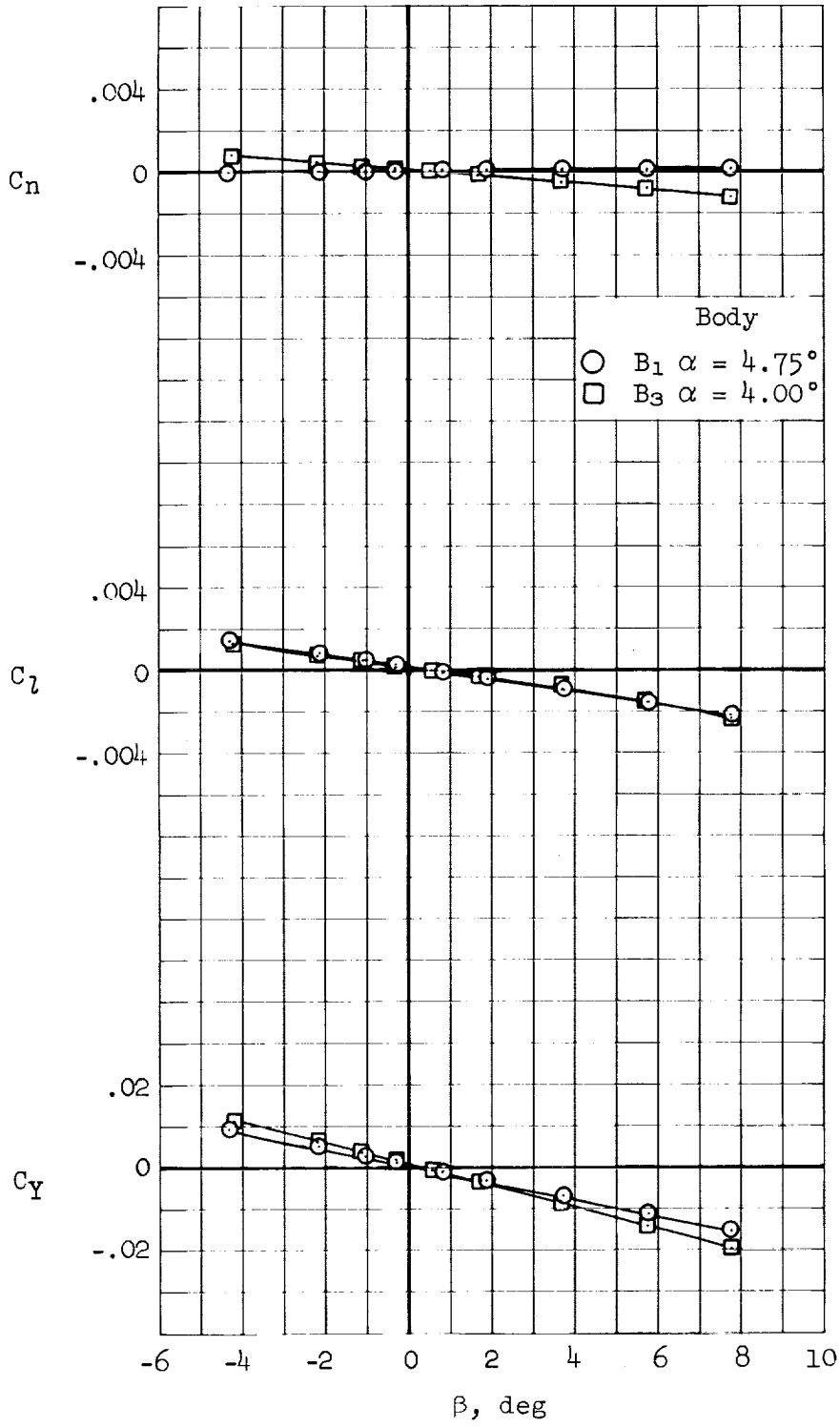

(e) M = 7.38

Figure 5.- Continued.

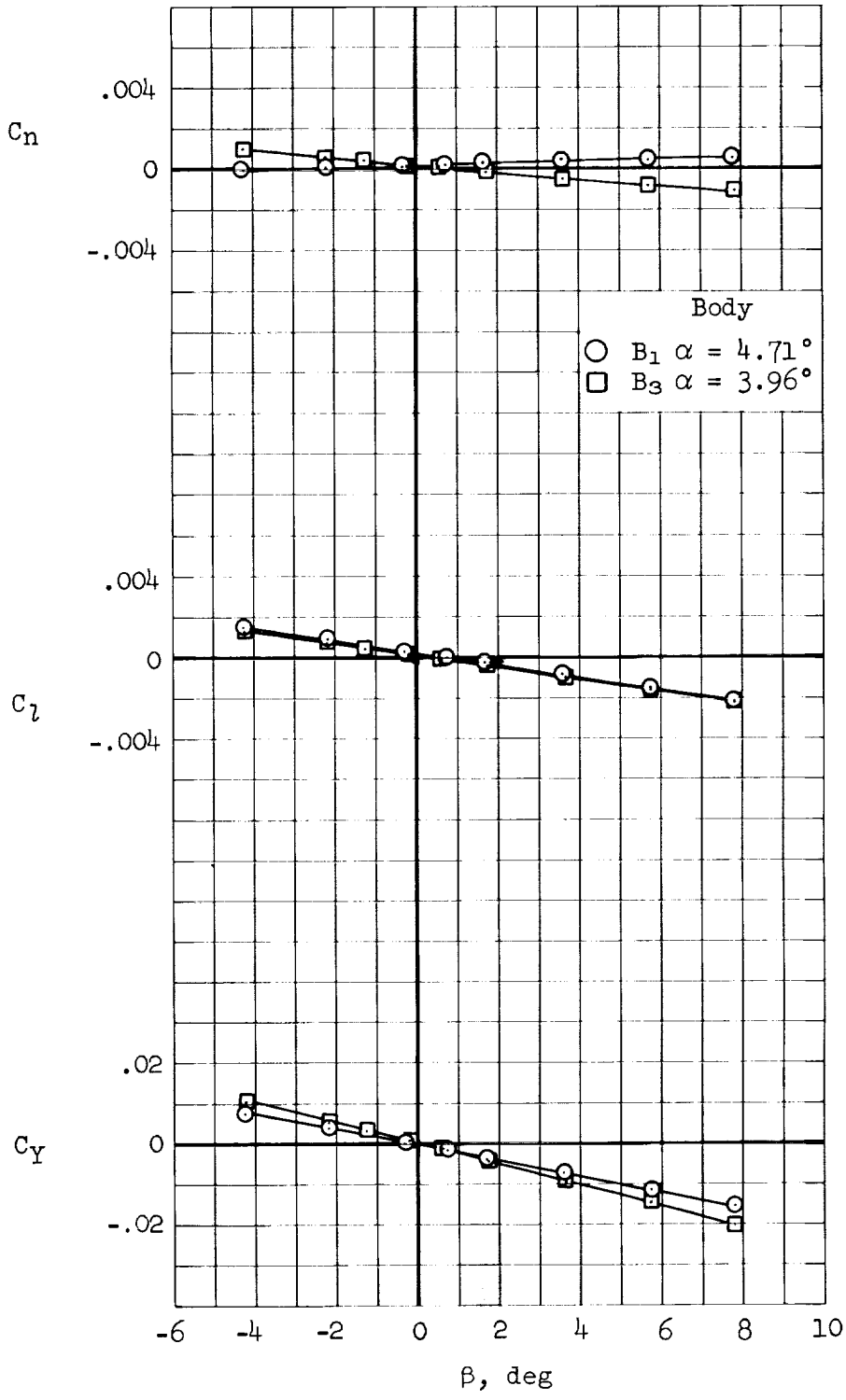

(f) M = 10.61

Figure 5.- Concluded.

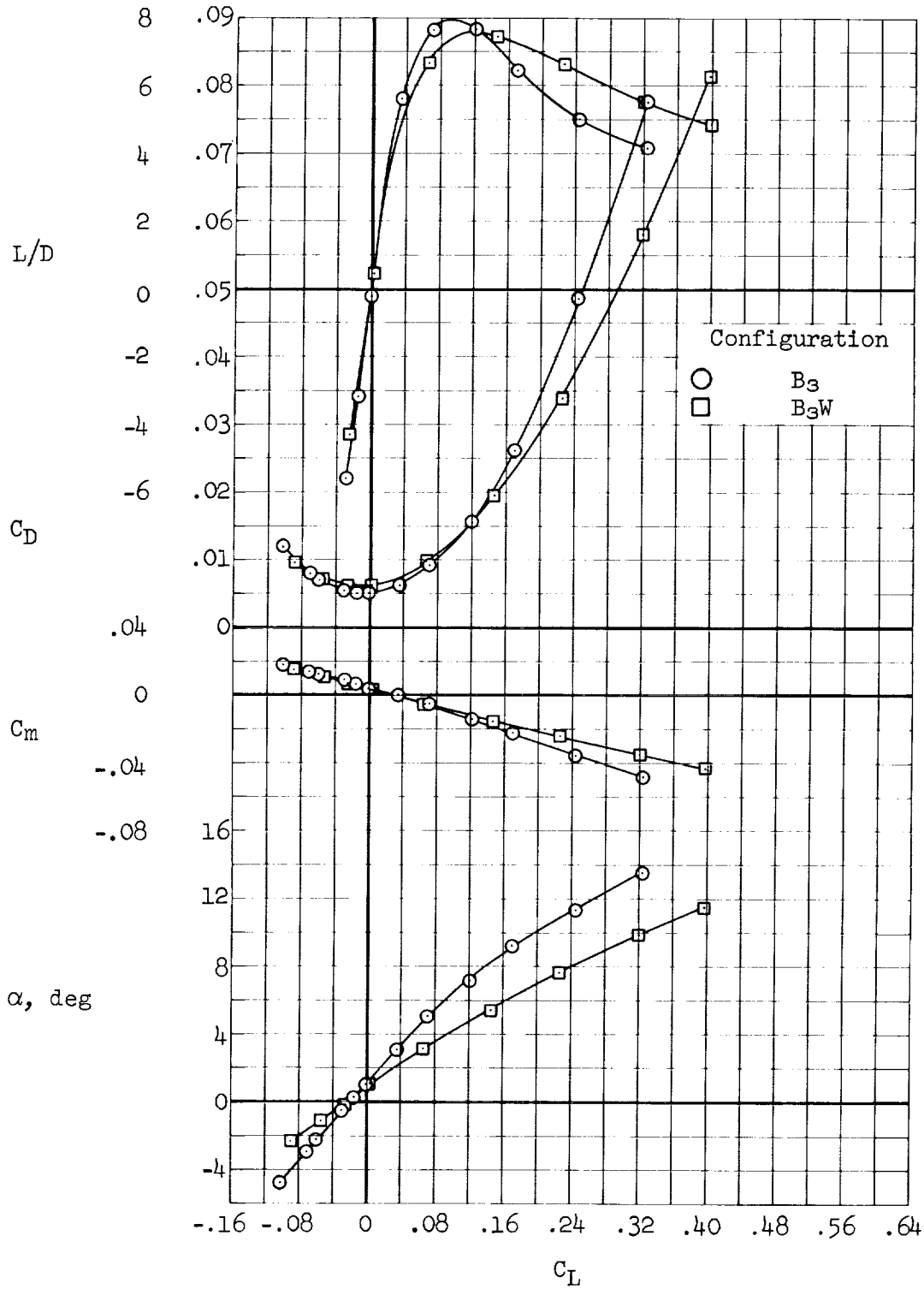

(a) M = 0.65

Figure 6.- Effect of wings on the longitudinal aerodynamic characteristics of the alternate sweep configuration.

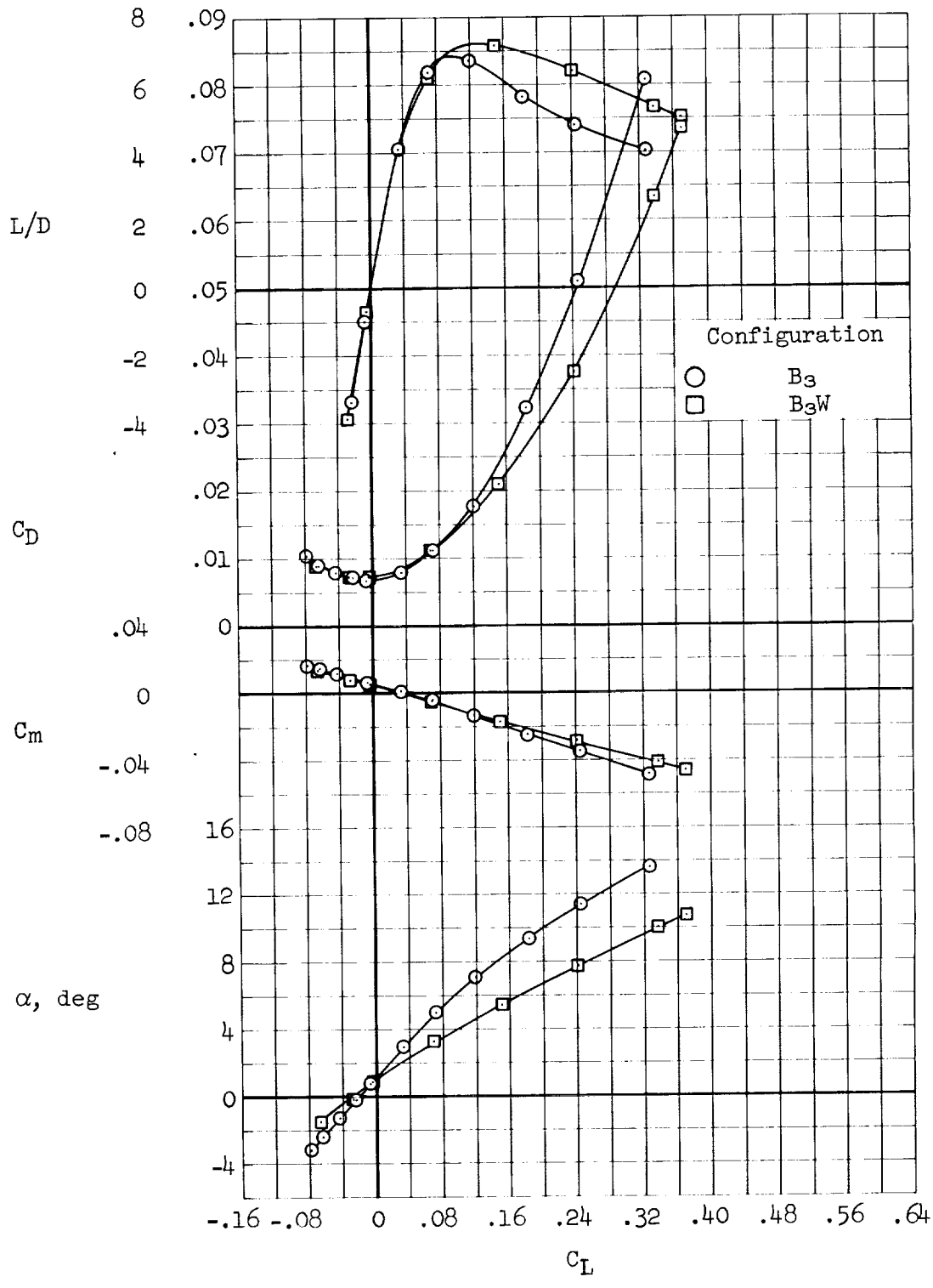

(b) M = 0.80

Figure 6.- Continued.

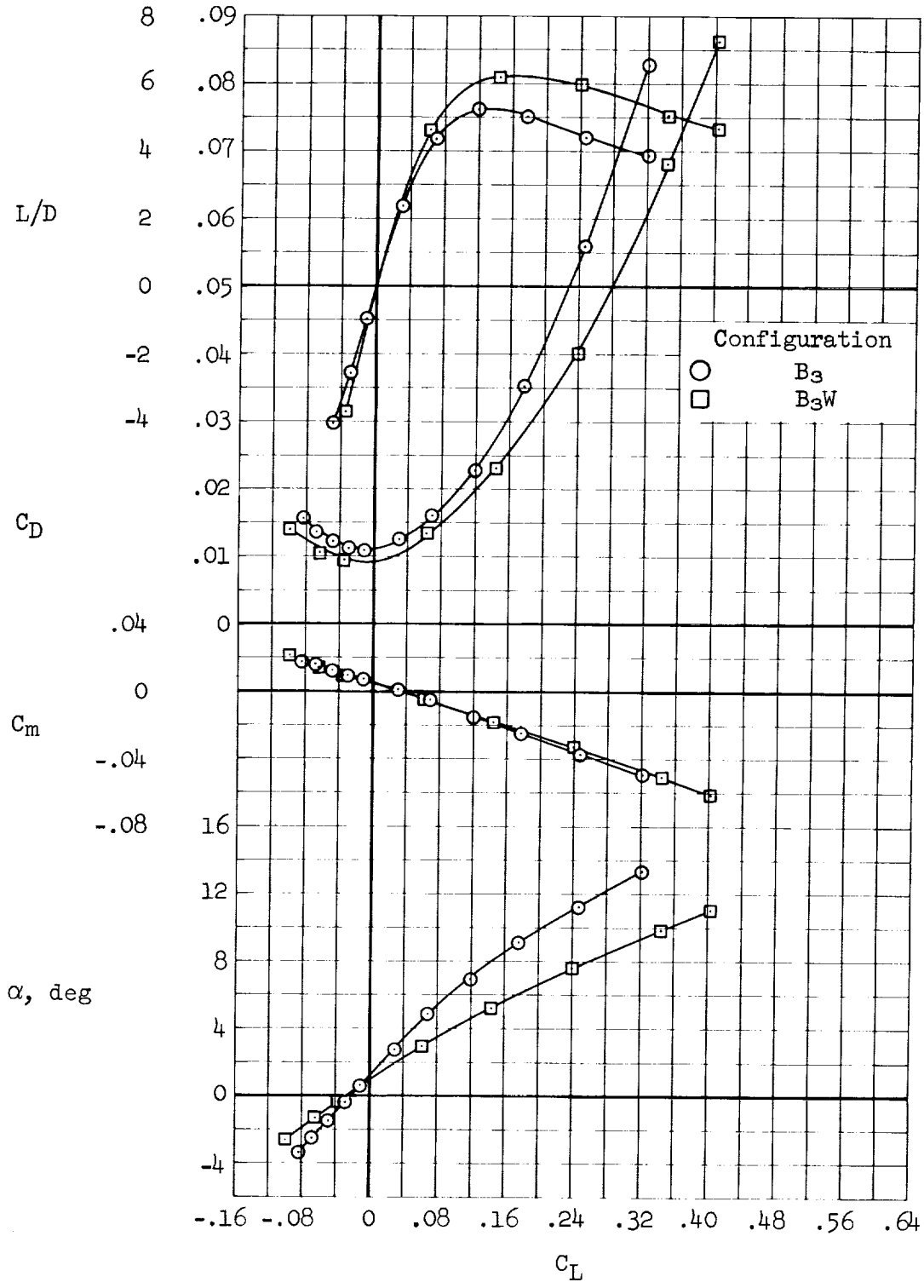

(c) M = 0.90

Figure 6.- Continued.

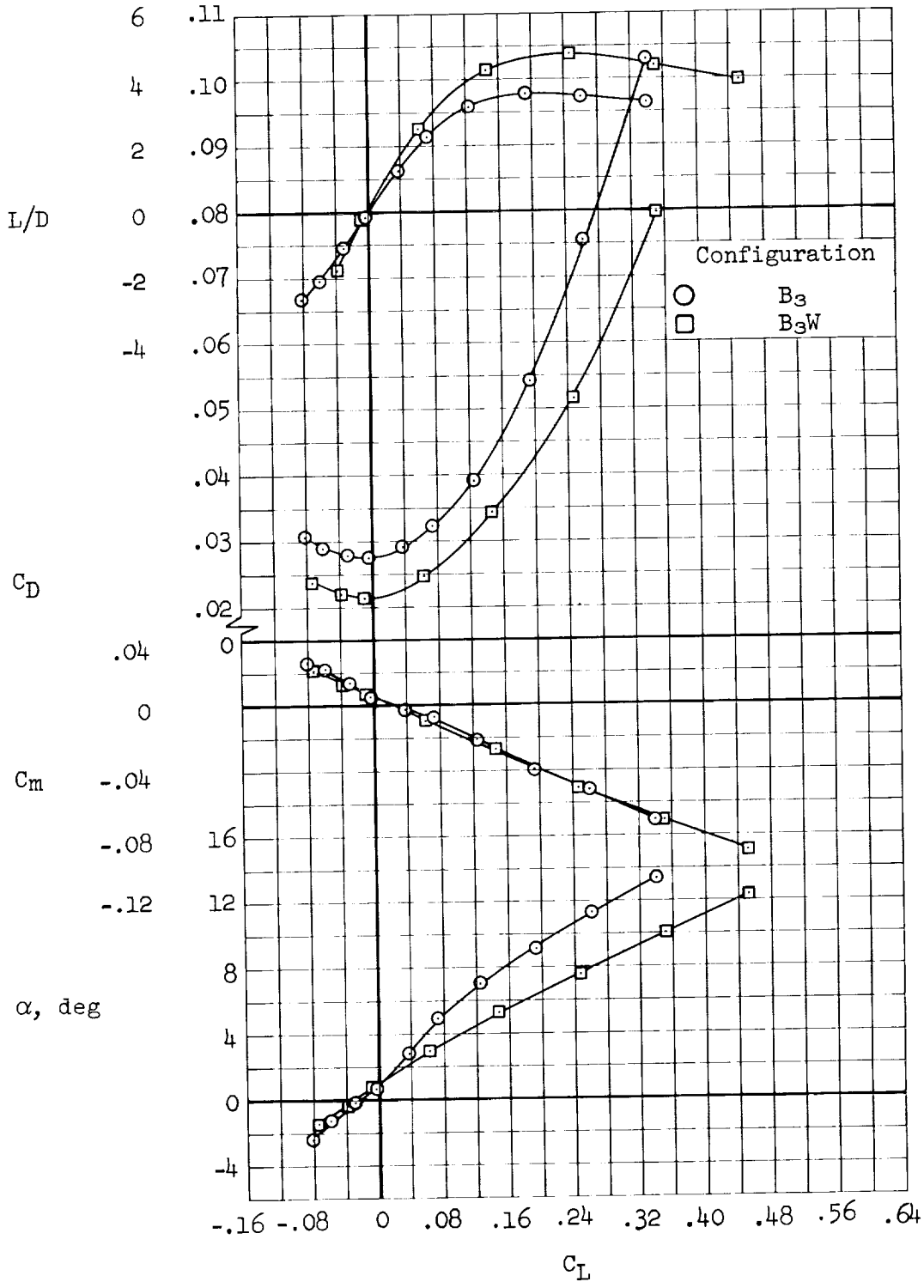

(d) M = 1.10

Figure 6.- Continued.

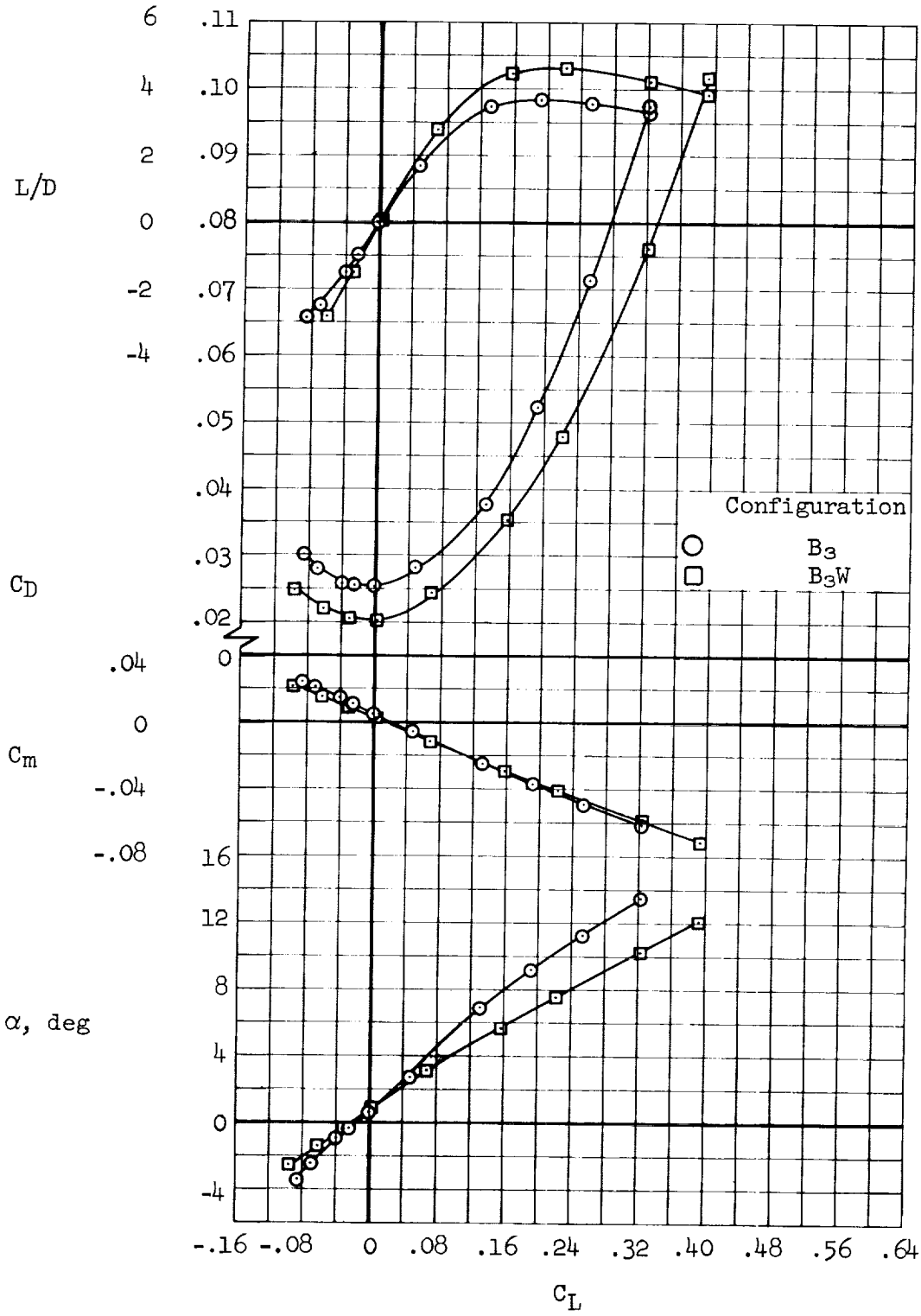

(e) M = 1.30

Figure 6.- Continued.

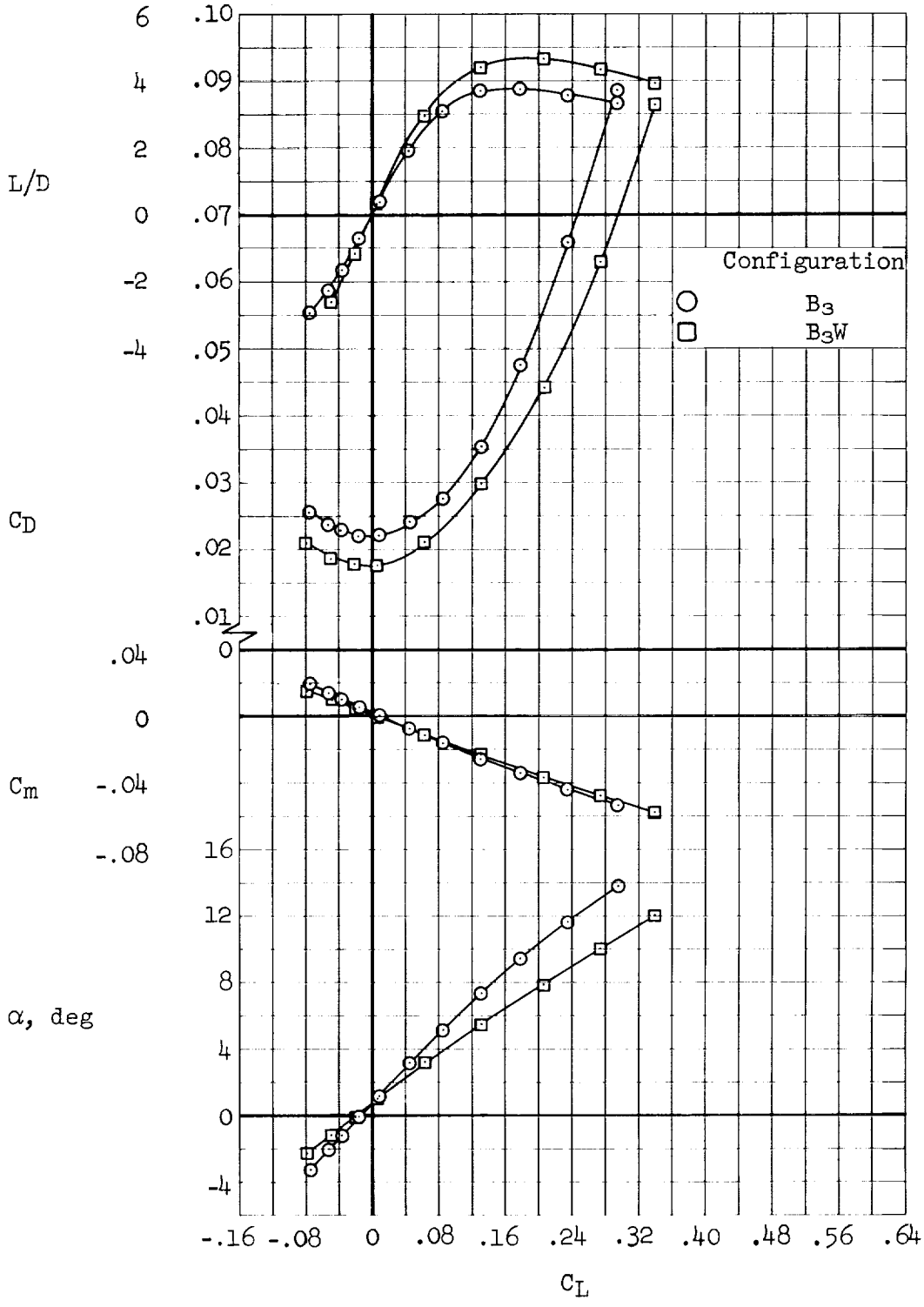

(f) M = 1.60

Figure 6.- Continued.

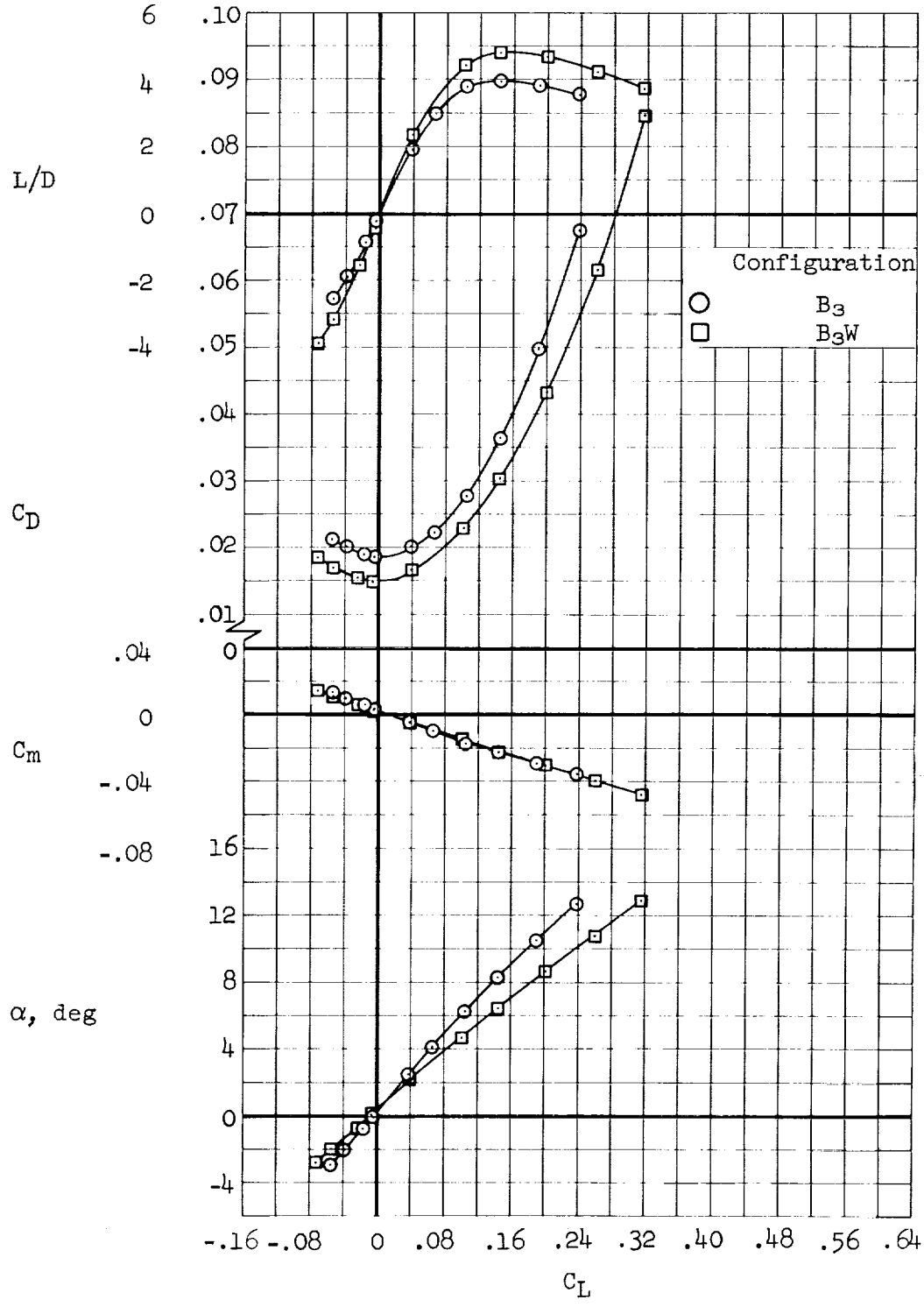

(g) M = 2.00

Figure 6.- Continued.

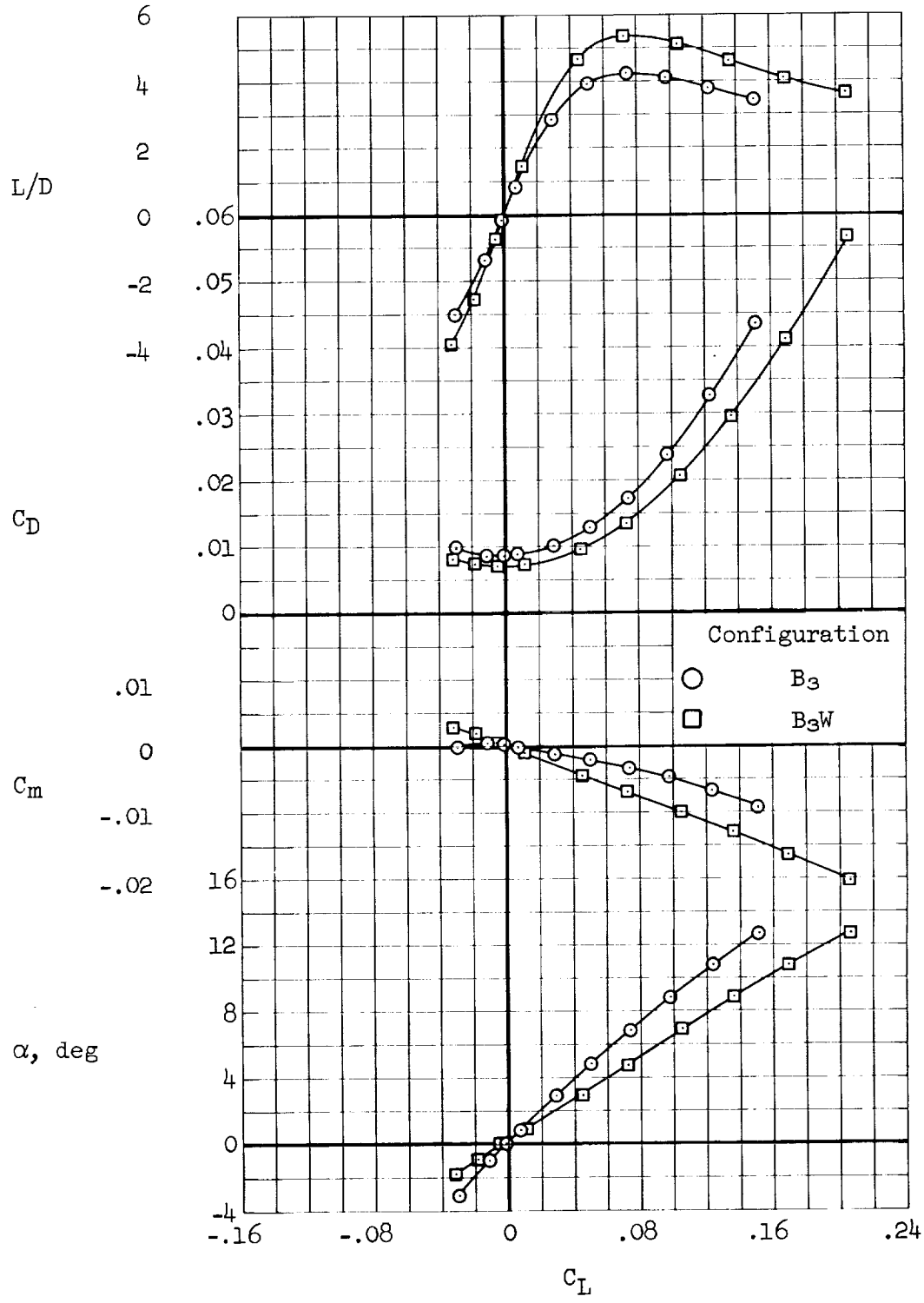

(h) M = 5.37

Figure 6.- Continued.

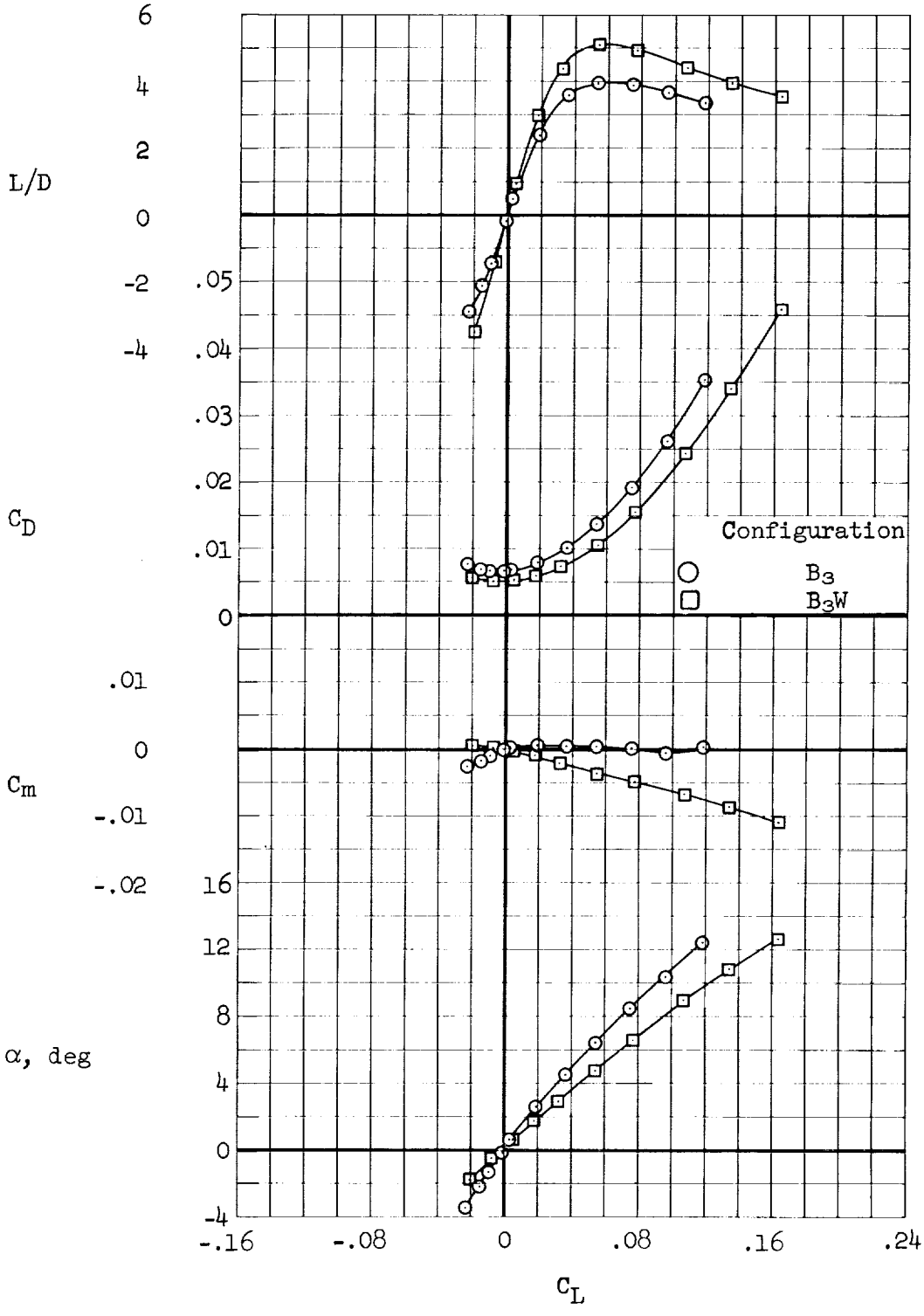

(i) M = 7.38

Figure 6.- Continued.

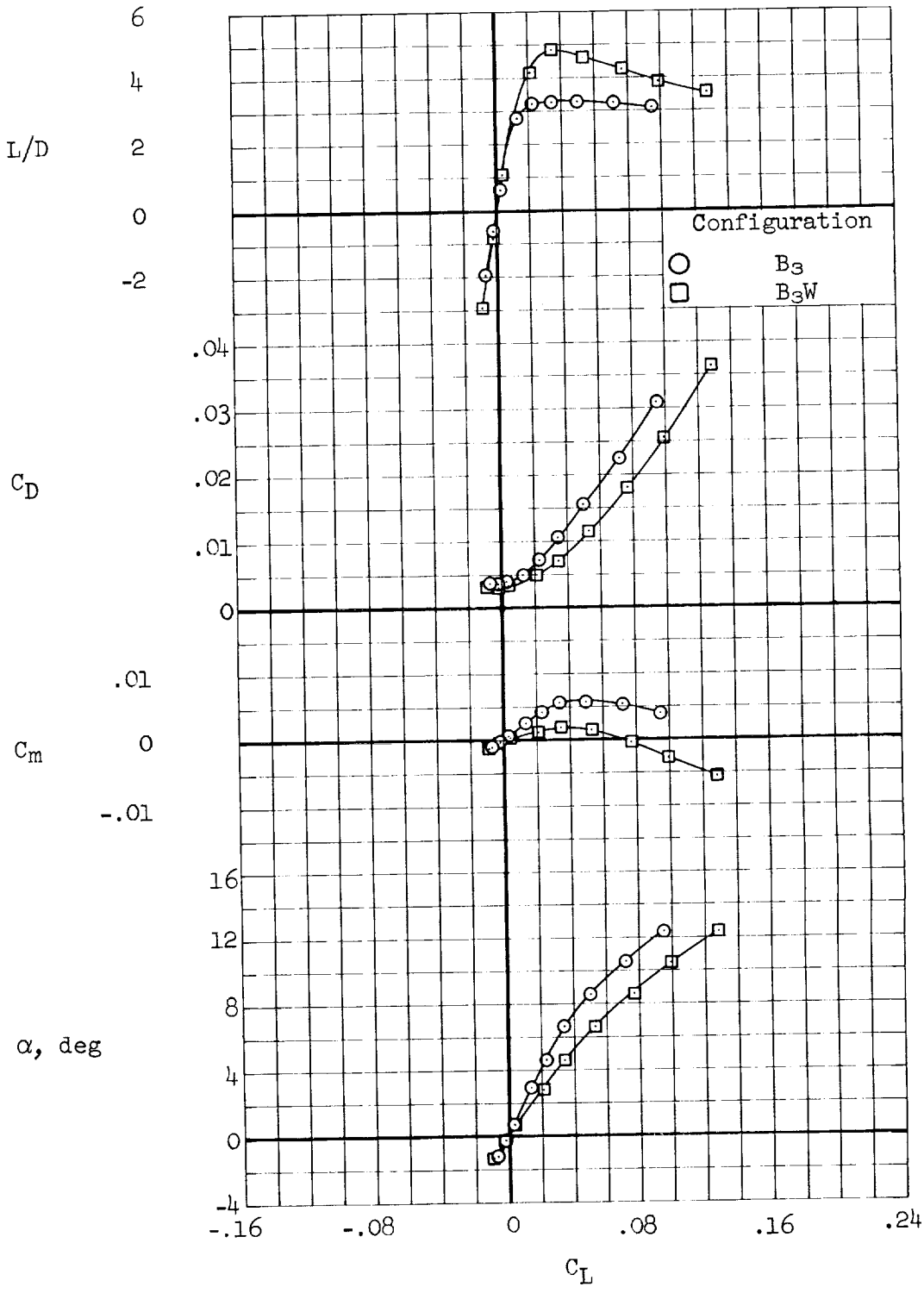

(j) M = 10.61

Figure 6.- Concluded.

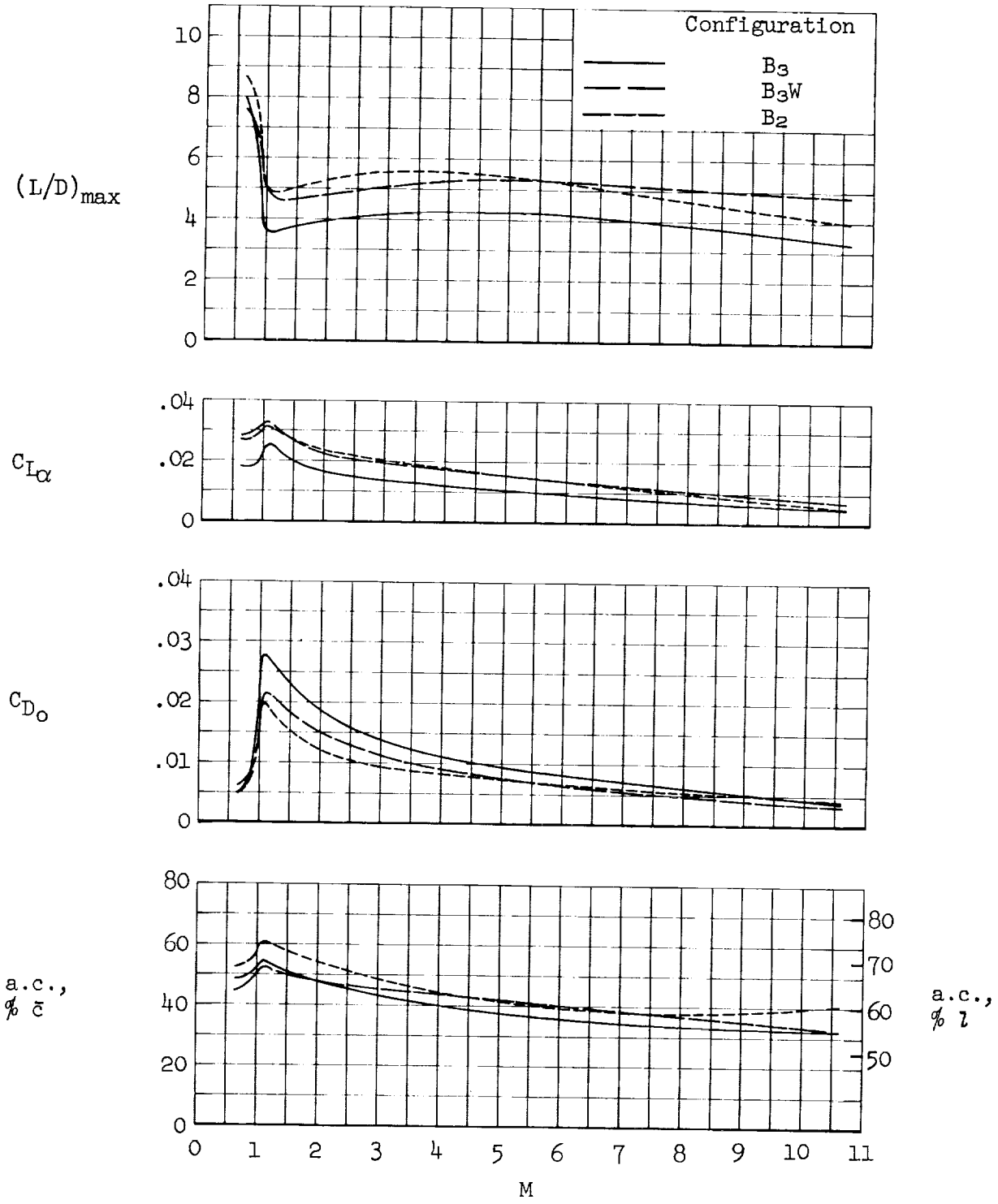

Figure 7.- Variation with Mach number of the effect of wings on the longitudinal aerodynamic characteristics of the alternate sweep configuration.

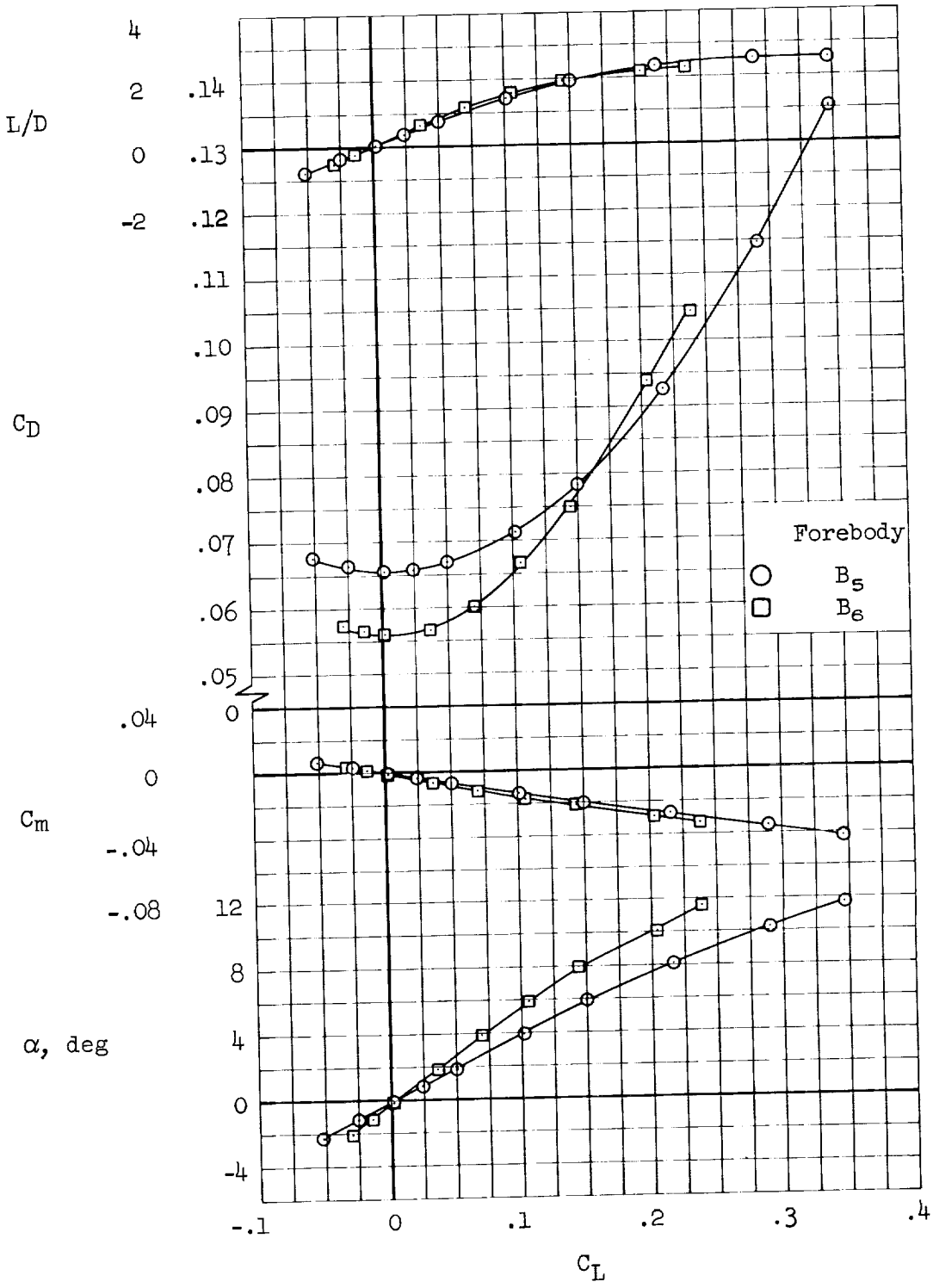

(a) M = 0.65

Figure 8.- Longitudinal aerodynamic characteristics of the forebodies of the nominal and alternate sweep configurations.

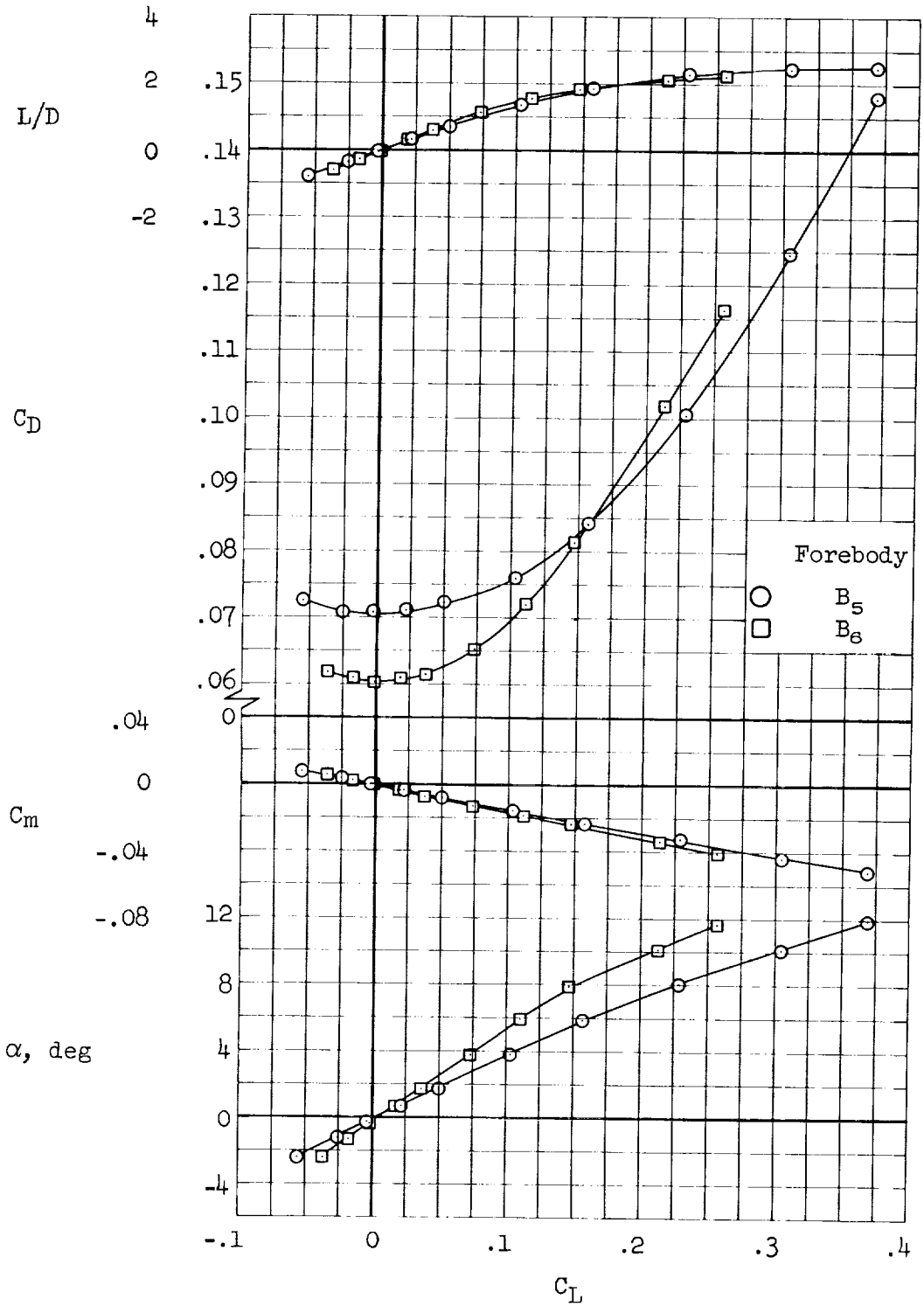

(b) M = 0.80

Figure 8.- Continued.

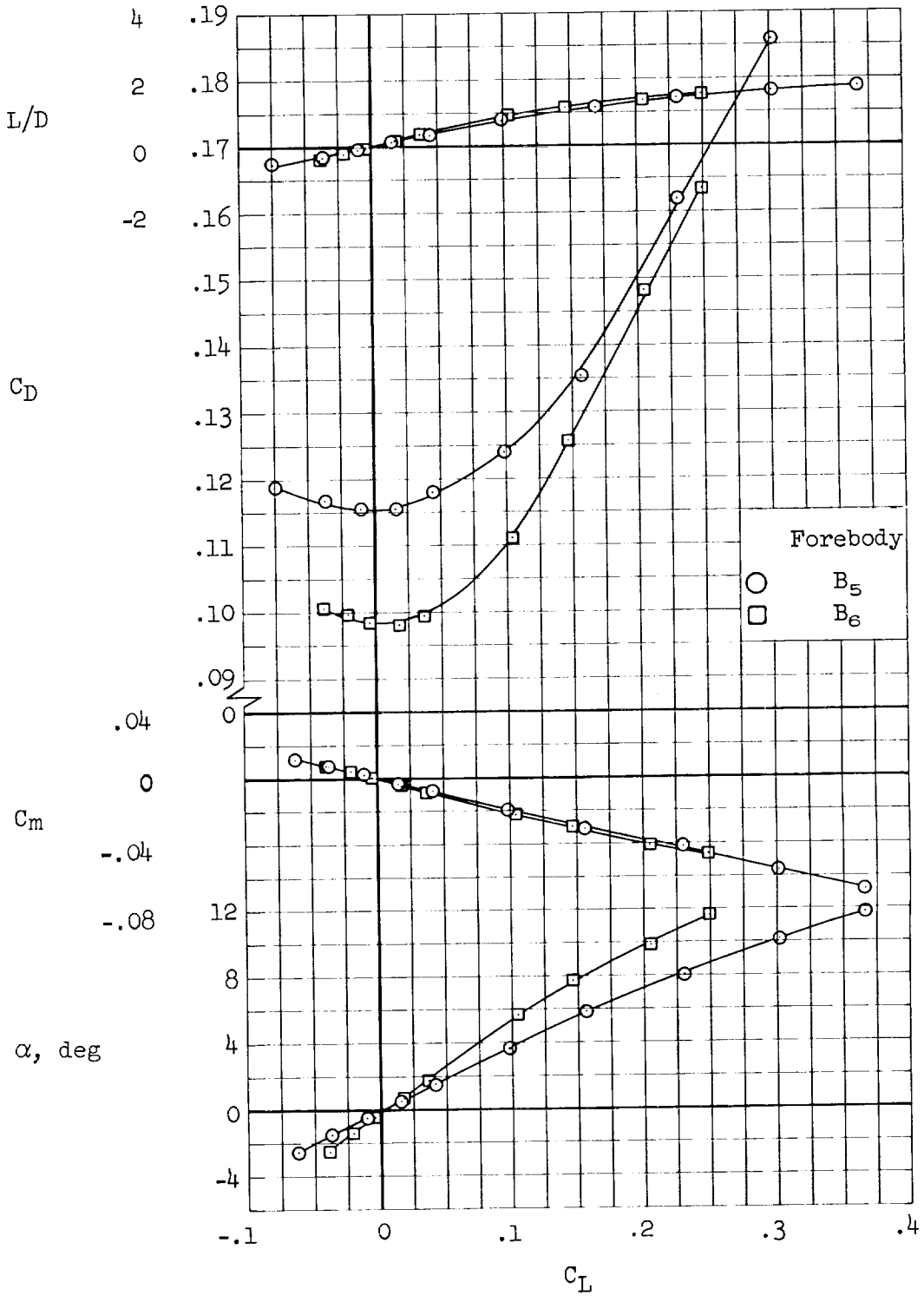

(c) M = 1.10

Figure 8.- Continued.

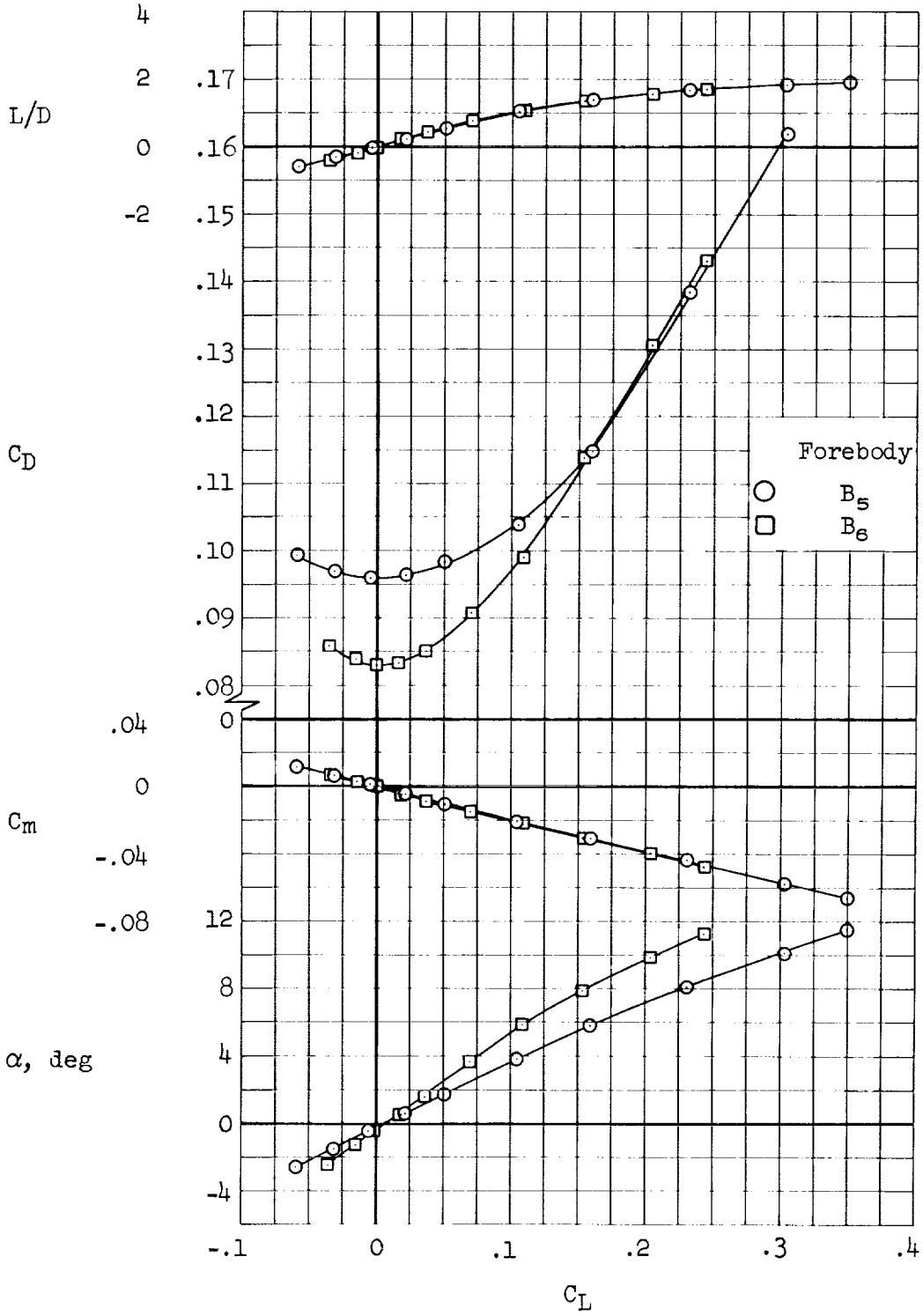

(d) M = 1.30

Figure 8.- Continued.

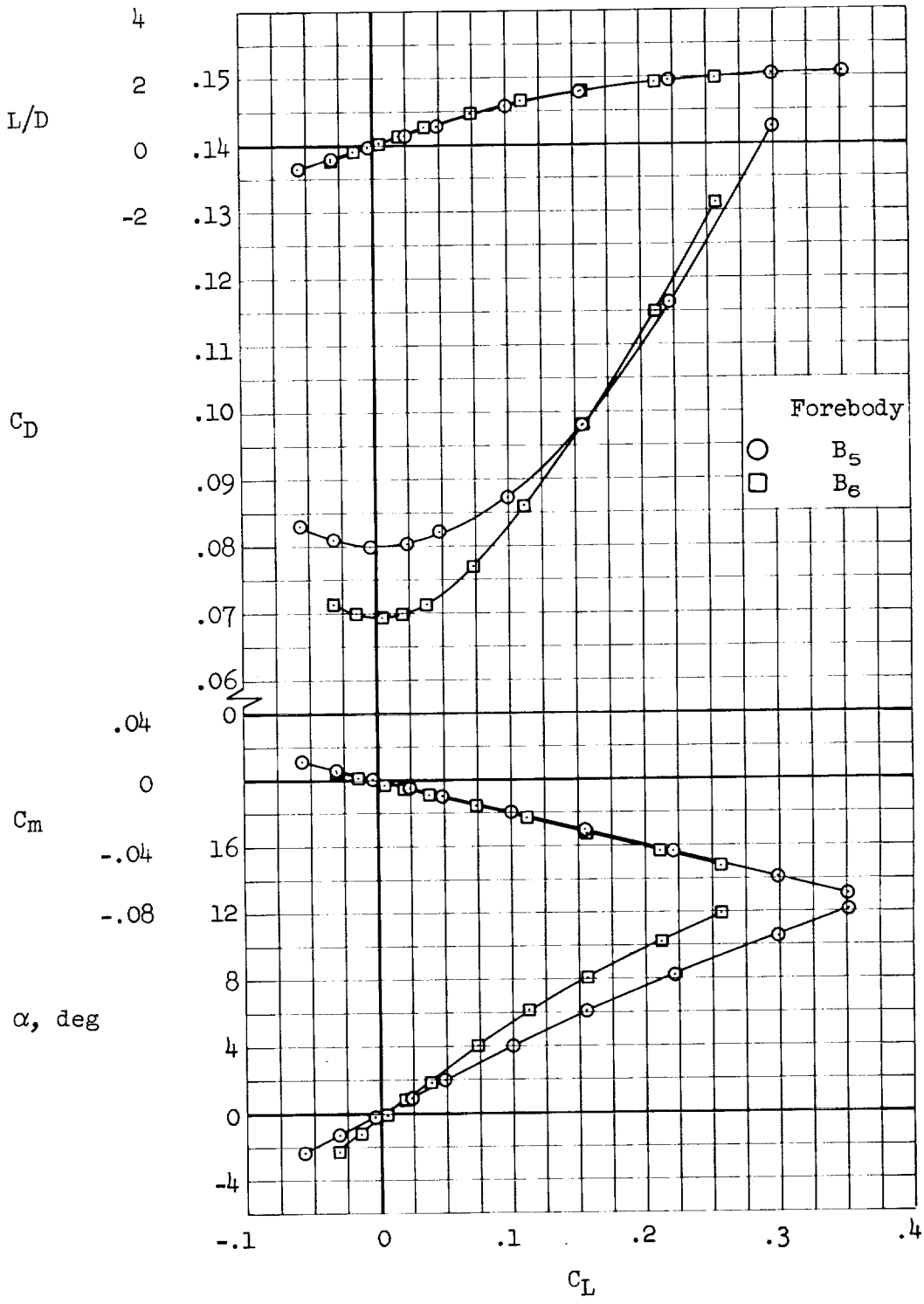

(e) M = 1.60

Figure 8.- Continued.

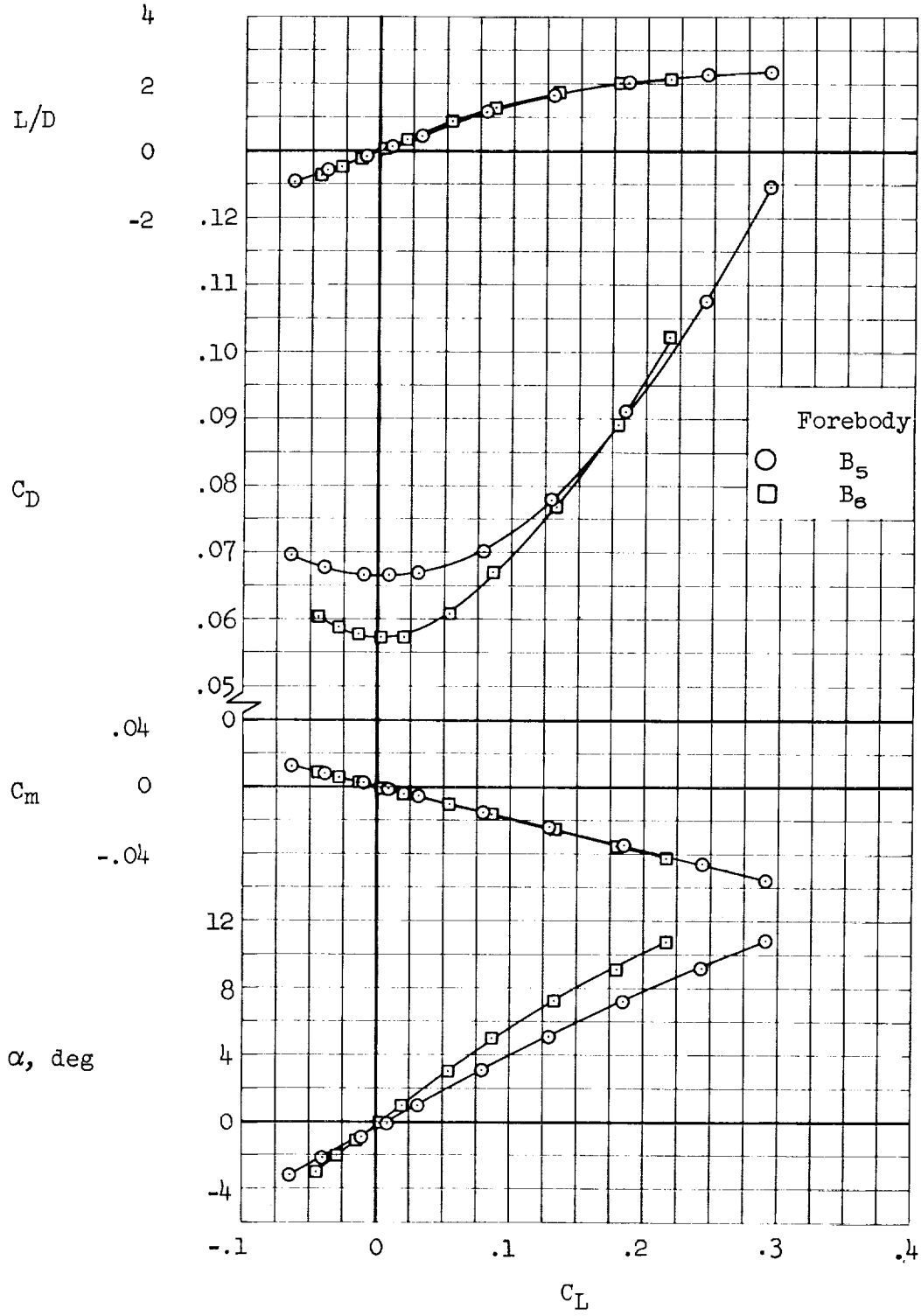

(f) M = 2.00

Figure 8.- Continued.

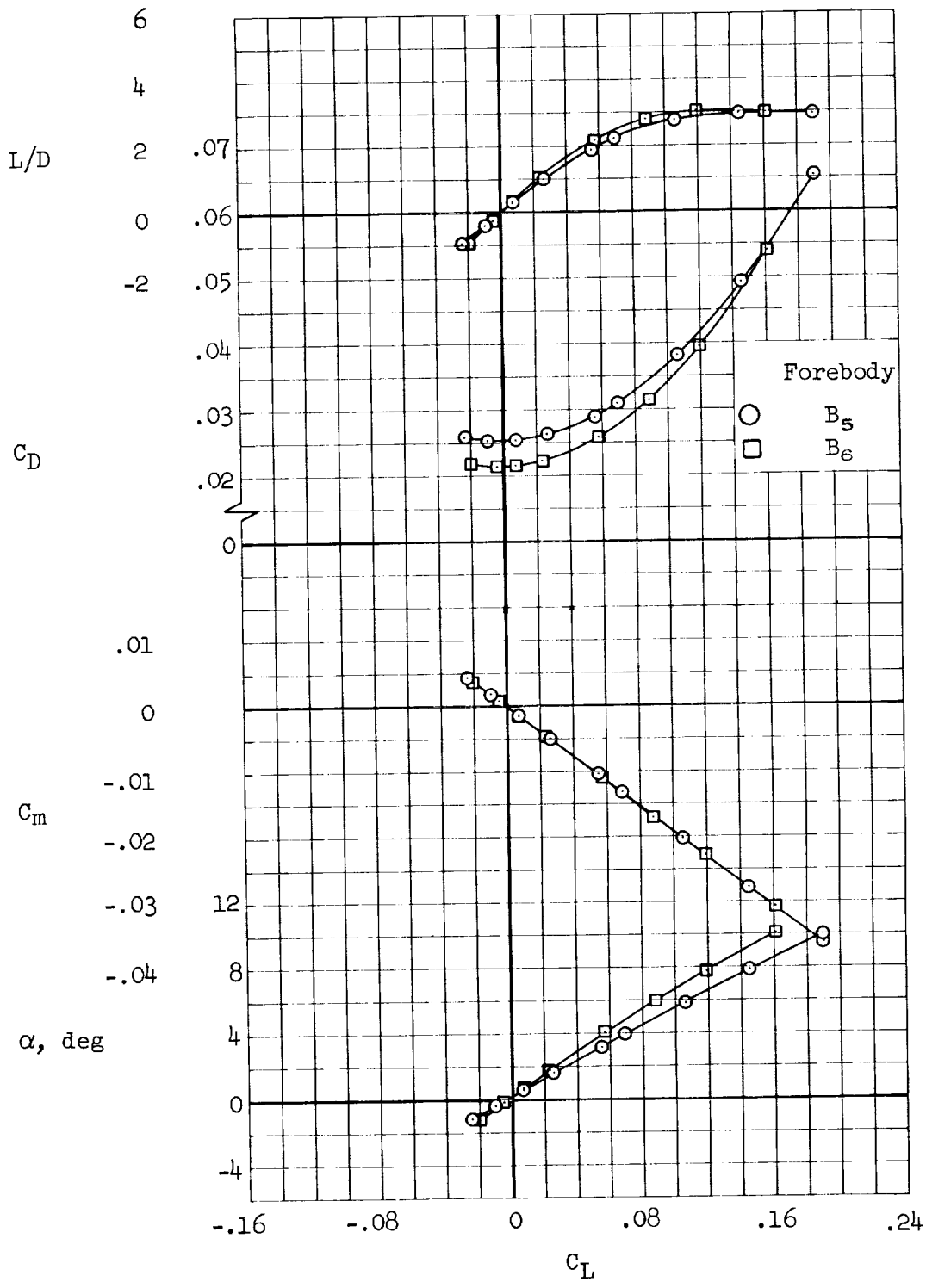

(g) M = 5.37

Figure 8.- Continued.

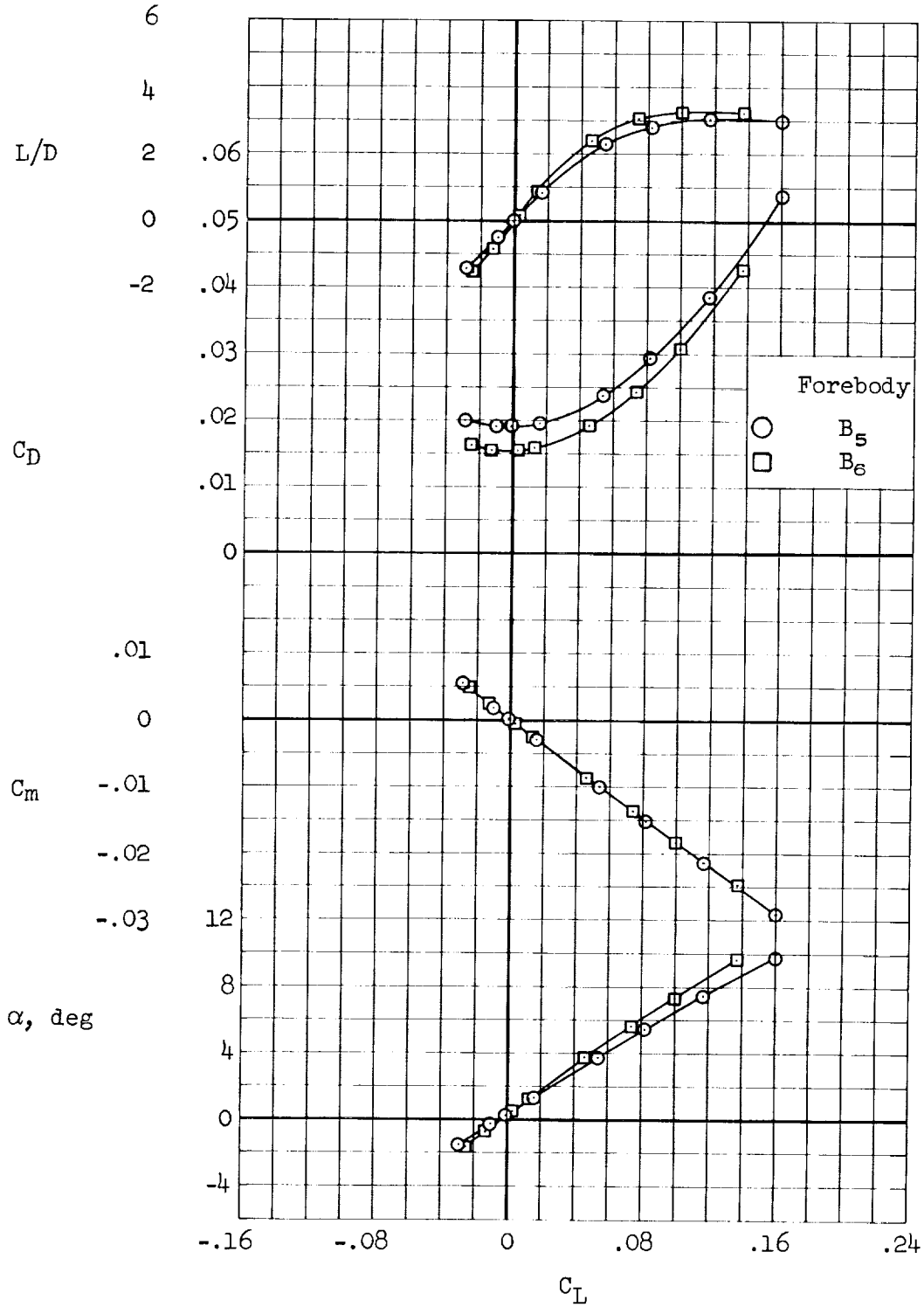

(h) M = 7.38

Figure 8.- Continued.

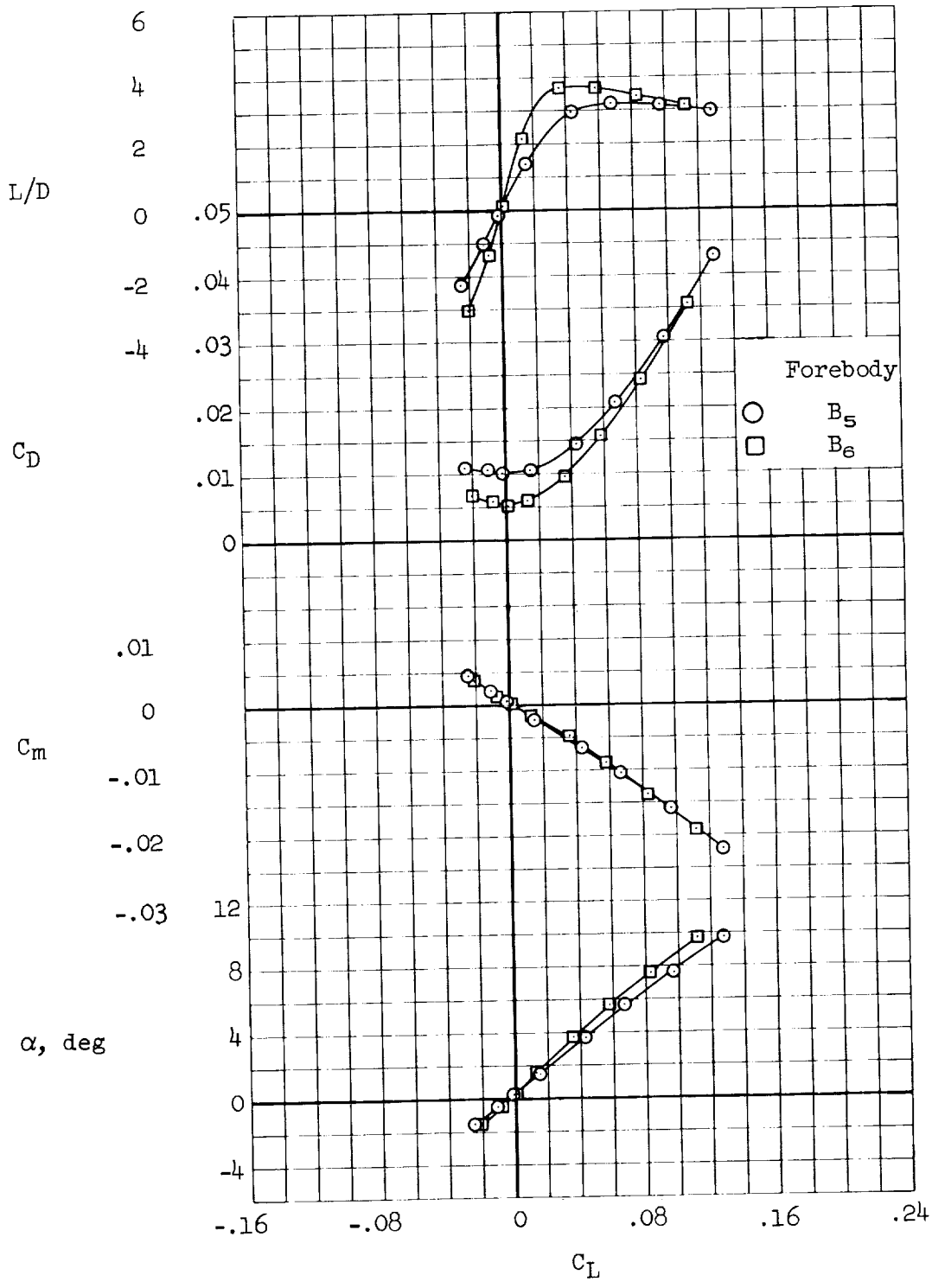

(i) M = 10.61

Figure 8.- Concluded.

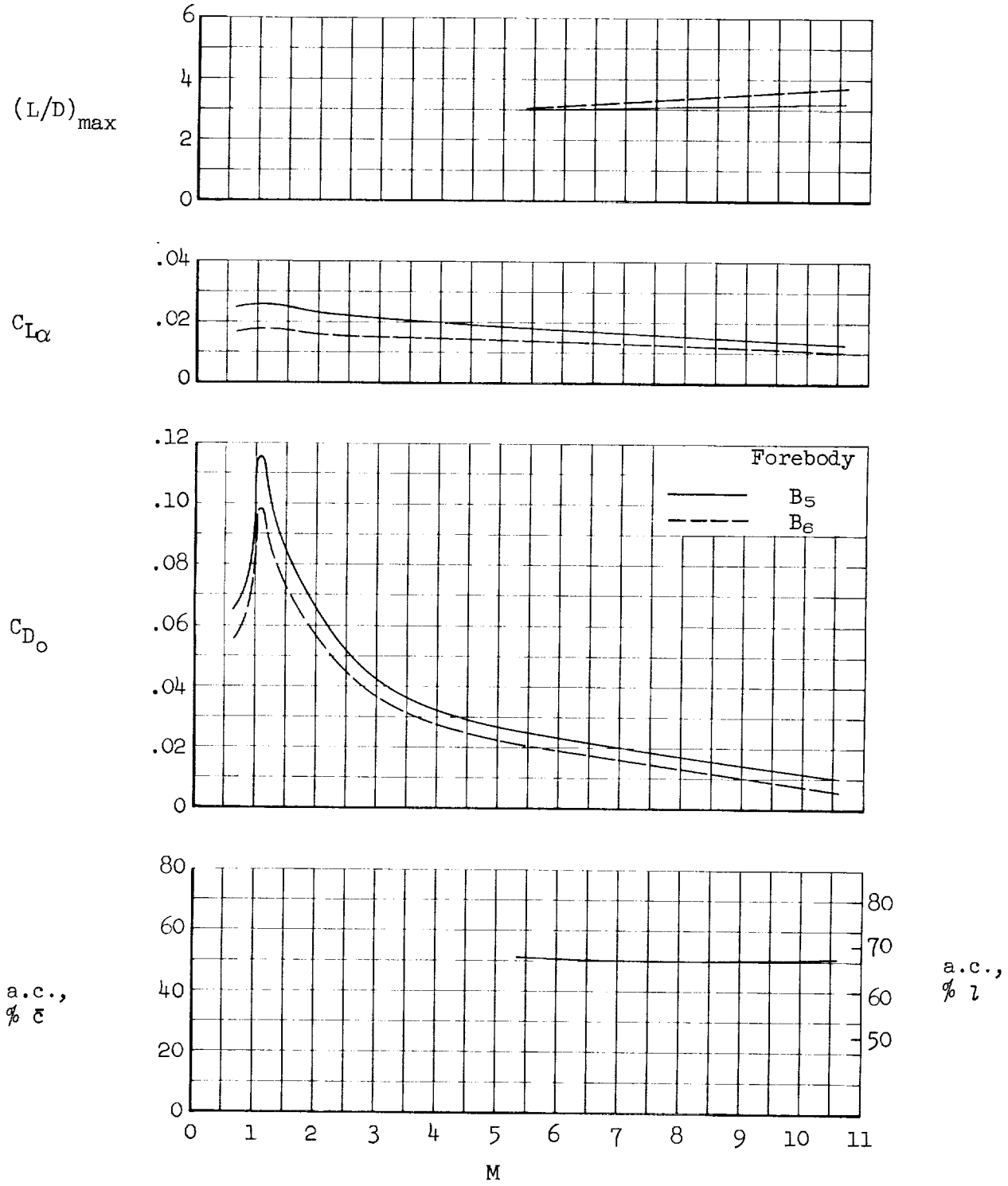

Figure 9.- Variation with Mach number of the longitudinal aerodynamic characteristics of the forebodies of the nominal and alternate sweep configurations.

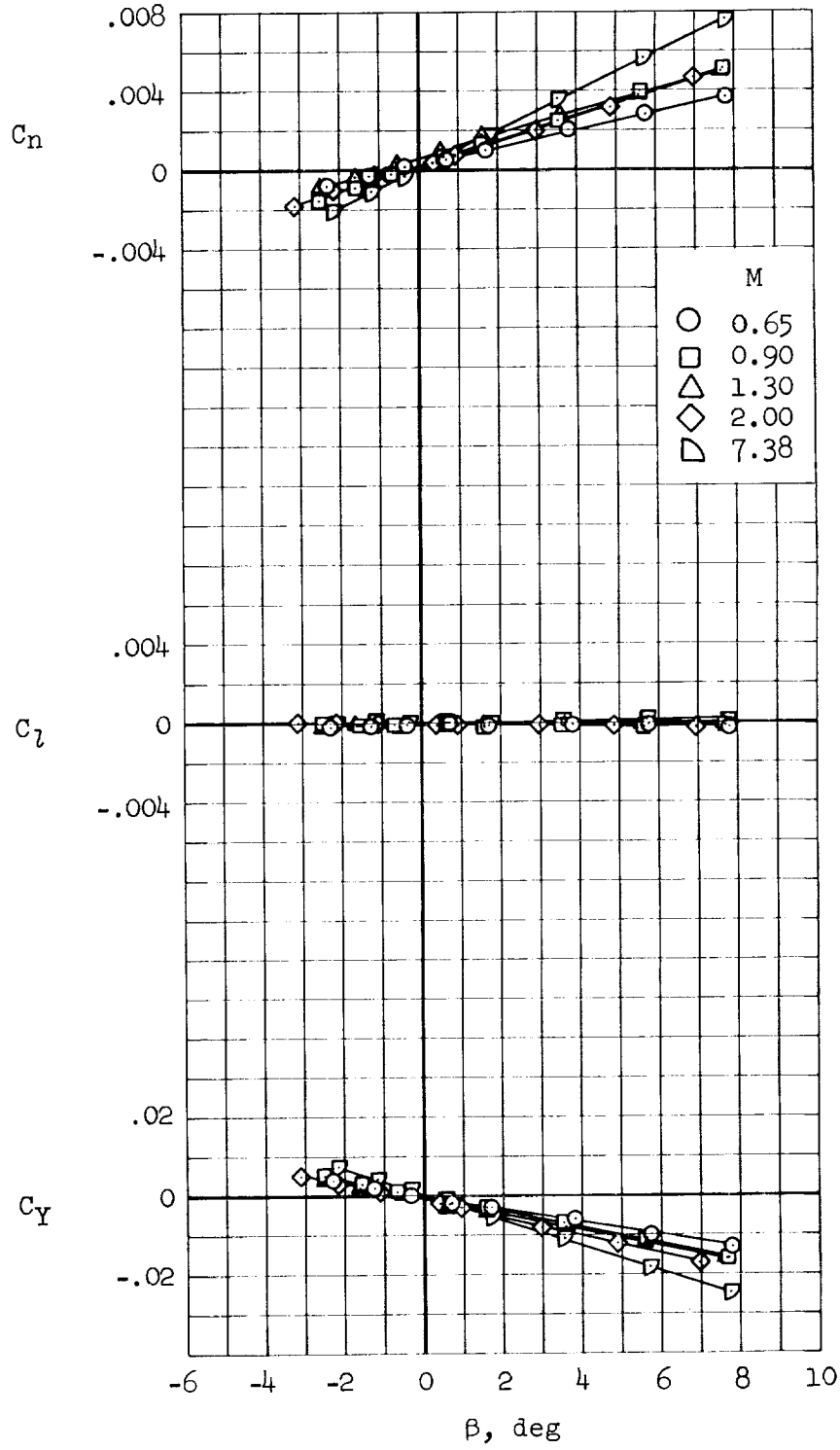

Figure 10.- Lateral-directional aerodynamic characteristics of the forebody of the nominal configuration; $\alpha = 0°$.

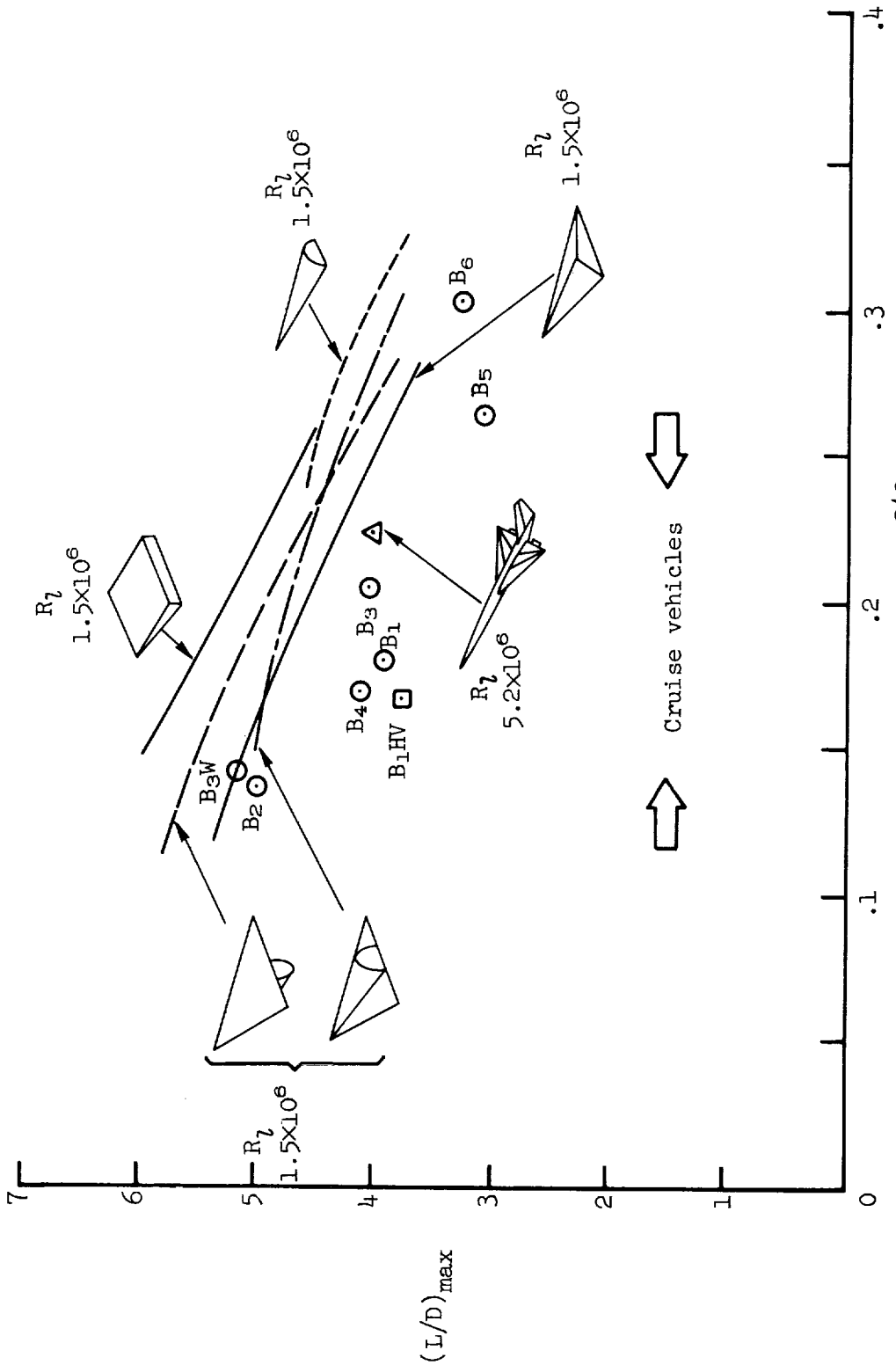

Figure 11.- $(L/D)_{max}$ for hypersonic configurations untrimmed in wind tunnels at M = 6.8 with laminar boundary layers.

NASA-Langley, 1972 —— 1 A-4297